presented here to give the most information about Tec interactors along with the appropriate level of experimental confidence.

HIF-1α, identified as a Tec interactor in this study, is an important mediator of adenosine nucleoside-induced neuroprotection in hypoxia-stimulated PC12 cells (34). Since Tec is activated by adenosine nucleotide stimulation in cardiomyocytes, it may participate in HIF-1α signaling during cardiac protection. Another interactor, CDC37, is an emerging heat shock protein 90 cochaperone whose client proteins are predominantly kinases (20). Also among the interactors we found was Rho kinase 1 (ROCK1), an immediate downstream kinase effector of RhoA GTPase. A recent knockout study (33) has indicated a critical role for ROCK1 in reactive fibrosis during pressure-overload hypertrophy. The specifics of how Tec may contribute to this process are unclear, but this observation is consistent with Tec's proliferative role in cell signaling and its abundant expression in fibroblasts. Finally, we found many structural proteins, such as ankyrin, spectrin, and clathrin, and many muscle contraction-associated proteins.

To mine for bioinformatic insights into the Tec subproteome, we examined how the physical-chemical properties of Tec interactors compare with the entire tandem MS-detectable proteome (i.e., the IPI database). The distributions of Tec interactors were not dramatically different from the IPI database for the metrics of molecular weight, isoelectric focusing point, and hydropathy score; however, Tec interactors differed significantly from the IPI database proteome in the area of protein disorder (Fig. 6), in which the Tec subproteome was populated by a significant number of proteins with extensive regions of disorder. Some investigators (29) have postulated that protein disorder is correlated with multifunctionality for protein interaction surfaces–the exact type used in signal transduction. It is worthwhile to note that Src (a homologous tyrosine kinase from a different family) and CDC27 (a Tec interactor identified in this study) subproteomes also had similar bias toward disorder.

We recognize that some of the most interesting aspects of the subproteome of Tec-associated signaling proteins remain unknown, including how it changes with stimulation and subcellular location. Indeed, these end points are the focus of ongoing work. However, the present study presents the first nonbiased analysis of Tec interactors in any cell type and sets the groundwork for the future investigation of cell- and stimulus-specific changes. Furthermore, we presented a rigorous and detailed methodological description of how protein interactions were determined (and false positives ruled out), which will inform future investigations of Tec and other signaling proteins via proteomics.

Summary and outlook. This study demonstrates the activation of endogenous Tec tyrosine kinase in mouse cardiac cells, illustrating similarities and differences with other Tec family members (Bmx in particular) as well as other nonreceptor tyrosine kinases from other protein families in myocardial ischemia and protection. This investigation provides the first global map of Tec-interacting proteins in any cell type. A model that emerges from this and other work is one in which a negative regulatory process (such as a tyrosine phosphatase) physically interacts with Tec kinase in an autoregulatory mechanism (Fig. 7) (25). Release from this cycle by stress stimuli allows Tec to associate with lipid membranes and regulate target proteins. Future studies will be necessary to test this model in detail in cardiac myocytes as well as to reveal the nuances of how Tec signals to different in vivo cellular targets.

GRANTS

This study was supported by National Heart, Lung, and Blood Institute (NHLBI) Grants HL-087132 and HL-096041 (to T. M. Vondriska), HL-088640 (to E. Stefani), and HL-080111 (to P. Ping) and the Laubisch Endowment of the University of California-Los Angeles (to T. M. Vondriska). M. J. Zhang received a scholarship from the University of California-Los Angeles Undergraduate Research Center. S. Franklin is the recipient of NHLBI Ruth Kirschstein Postdoctoral Fellowship F32-HL-091673.

DISCLOSURES

No conflicts of interest, financial or otherwise, are declared by the author(s).

REFERENCES

1. **Aoki N, Ueno S, Mano H, Yamasaki S, Shiota M, Miyazaki H, Yamaguchi-Aoki Y, Matsuda T, Ullrich A.** Mutual regulation of protein-tyrosine phosphatase 20 and protein-tyrosine kinase Tec activities by tyrosine phosphorylation and dephosphorylation. *J Biol Chem* 279: 10765–10775, 2004.
2. **Aranda B, Achuthan P, Alam-Faruque Y, Armean I, Bridge A, Derow C, Feuermann M, Ghanbarian AT, Kerrien S, Khadake J, Kerssemakers J, Leroy C, Menden M, Michaut M, Montecchi-Palazzi L, Neuhauser SN, Orchard S, Perreau V, Roechert B, van Eijk K, Hermjakob H.** The IntAct molecular interaction database in 2010. *Nucleic Acids Res* 38: D525–D531, 2010.
3. **Berglund L, Bjorling E, Oksvold P, Fagerberg L, Asplund A, Szigyarto CA, Persson A, Ottosson J, Wernerus H, Nilsson P, Lundberg E, Sivertsson A, Navani S, Wester K, Kampf C, Hober S, Ponten F, Uhlen M.** A genecentric Human Protein Atlas for expression profiles based on antibodies. *Mol Cell Proteomics* 7: 2019–2027, 2008.
4. **Bony C, Roche S, Shuichi U, Sasaki T, Crackower MA, Penninger J, Mano H, Puceat M.** A specific role of phosphatidylinositol 3-kinase gamma. A regulation of autonomic Ca^{2+} oscillations in cardiac cells. *J Cell Biol* 152: 717–728, 2001.
5. **Eble DM, Strait JB, Govindarajan G, Lou J, Byron KL, Samarel AM.** Endothelin-induced cardiac myocyte hypertrophy: role for focal adhesion kinase. *Am J Physiol Heart Circ Physiol* 278: H1695–H1707, 2000.
6. **Fox AC, Reed GE, Glassman E, Kaltman AJ, Silk BB.** Release of adenosine from human hearts during angina induced by rapid atrial pacing. *J Clin Invest* 53: 1447–1457, 1974.
7. **Haendeler J, Berk BC.** Angiotensin II mediated signal transduction. Important role of tyrosine kinases. *Regul Pept* 95: 1–7, 2000.
8. **Hakim ZS, DiMichele LA, Rojas M, Meredith D, Mack CP, Taylor JM.** FAK regulates cardiomyocyte survival following ischemia/reperfusion. *J Mol Cell Cardiol* 46: 241–248, 2009.
9. **Hattori R, Otani H, Uchiyama T, Imamura H, Cui J, Maulik N, Cordis GA, Zhu L, Das DK.** Src tyrosine kinase is the trigger but not the mediator of ischemic preconditioning. *Am J Physiol Heart Circ Physiol* 281: H1066–H1074, 2001.
10. **He Y, Luo Y, Tang SB, Rajantie I, Salven P, Heil M, Zhang R, Luo DH, Li XH, Chi HB, Yu J, Carmeliet P, Schaper W, Sinusas AJ, Sessa WC, Alitalo K, Min W.** Critical function of Bmx/Etk in ischemia-mediated arteriogenesis and angiogenesis. *J Clin Invest* 116: 2344–2355, 2006.
11. **Hirotani S, Higuchi Y, Nishida K, Nakayama H, Yamaguchi O, Hikoso S, Takeda T, Kashiwase K, Watanabe T, Asahi M, Taniike M, Tsujimoto I, Matsumura Y, Sasaki T, Hori M, Otsu K.** Ca^{2+}-sensitive tyrosine kinase Pyk2/CAK beta-dependent signaling is essential for G-protein-coupled receptor agonist-induced hypertrophy. *J Mol Cell Cardiol* 36: 799–807, 2004.
12. **Kawakami Y, Hartman SE, Kinoshita E, Suzuki H, Kitaura J, Yao L, Inagaki N, Franco A, Hata D, Maeda-Yamamoto M, Fukamachi H, Nagai H, Kawakami T.** Terreic acid, a quinone epoxide inhibitor of Bruton's tyrosine kinase. *Proc Natl Acad Sci USA* 96: 2227–2232, 1999.
13. **Mano H, Yamashita Y, Miyazato A, Miura Y, Ozawa K.** Tec protein-tyrosine kinase is an effector molecule of Lyn protein-tyrosine kinase. *FASEB J* 10: 637–642, 1996.

14. **Mitchell-Jordan SA, Holopainen T, Ren S, Wang S, Warburton S, Zhang MJ, Alitalo K, Wang Y, Vondriska TM.** Loss of Bmx nonreceptor tyrosine kinase prevents pressure overload-induced cardiac hypertrophy. *Circ Res* 103: 1359–1362, 2008.
15. **Mottet D, Dumont V, Deccache Y, Demazy C, Ninane N, Raes M, Michiels C.** Regulation of hypoxia-inducible factor-1alpha protein level during hypoxic conditions by the phosphatidylinositol 3-kinase/Akt/glycogen synthase kinase 3beta pathway in HepG2 cells. *J Biol Chem* 278: 31277–31285, 2003.
16. **O'Connell TD, Rodrigo MC, Simpson PC.** Isolation and culture of adult mouse cardiac myocytes. *Methods Mol Biol* 357: 271–296, 2007.
17. **Patel HH, Insel PA.** Lipid rafts and caveolae and their role in compartmentation of redox signaling. *Antioxid Redox Signal* 11: 1357–1372, 2009.
18. **Rajantie I, Ekman N, Iljin K, Arighi E, Gunji Y, Kaukonen J, Palotie A, Dewerchin M, Carmeliet P, Alitalo K.** Bmx tyrosine kinase has a redundant function downstream of angiopoietin and vascular endothelial growth factor receptors in arterial endothelium. *Mol Cell Biol* 21: 4647–4655, 2001.
19. **Schwartzberg PL, Finkelstein LD, Readinger JA.** TEC-family kinases: regulators of T-helper-cell differentiation. *Nat Rev Immunol* 5: 284–295, 2005.
20. **Smith JR, Workman P.** Targeting CDC37: an alternative, kinase-directed strategy for disruption of oncogenic chaperoning. *Cell Cycle* 8: 362–372, 2009.
21. **Takahashi-Tezuka M, Hibi M, Fujitani Y, Fukada T, Yamaguchi T, Hirano T.** Tec tyrosine kinase links the cytokine receptors to PI-3 kinase probably through JAK. *Oncogene* 14: 2273–2282, 1997.
22. **Takahashi N, Seko Y, Noiri E, Tobe K, Kadowaki T, Sabe H, Yazaki Y.** Vascular endothelial growth factor induces activation and subcellular translocation of focal adhesion kinase (p125FAK) in cultured rat cardiac myocytes. *Circ Res* 84: 1194–1202, 1999.
23. **Takano H, Tang XL, Qiu Y, Guo Y, French BA, Bolli R.** Nitric oxide donors induce late preconditioning against myocardial stunning and infarction in conscious rabbits via an antioxidant-sensitive mechanism. *Circ Res* 83: 73–84, 1998.
24. **Tang B, Mano H, Yi T, Ihle JN.** Tec kinase associates with c-kit and is tyrosine phosphorylated and activated following stem cell factor binding. *Mol Cell Biol* 14: 8432–8437, 1994.
25. **Tomlinson MG, Heath VL, Turck CW, Watson SP, Weiss A.** SHIP family inositol phosphatases interact with and negatively regulate the Tec tyrosine kinase. *J Biol Chem* 279: 55089–55096, 2004.
26. **Tomlinson MG, Kane LP, Su J, Kadlecek TA, Mollenauer MN, Weiss A.** Expression and function of Tec, Itk, and Btk in lymphocytes: evidence for a unique role for Tec. *Mol Cell Biol* 24: 2455–2466, 2004.
27. **Vondriska TM, Zhang J, Song C, Tang XL, Cao X, Baines CP, Pass JM, Wang S, Bolli R, Ping P.** Protein kinase C epsilon-Src modules direct signal transduction in nitric oxide-induced cardioprotection: complex formation as a means for cardioprotective signaling. *Circ Res* 88: 1306–1313, 2001.
28. **Wang G, Liem DA, Vondriska TM, Honda HM, Korge P, Pantaleon DM, Qiao X, Wang Y, Weiss JN, Ping P.** Nitric oxide donors protect murine myocardium against infarction via modulation of mitochondrial permeability transition. *Am J Physiol Heart Circ Physiol* 288: H1290–H1295, 2005.
29. **Ward JJ, Sodhi JS, McGuffin LJ, Buxton BF, Jones DT.** Prediction and functional analysis of native disorder in proteins from the three kingdoms of life. *J Mol Biol* 337: 635–645, 2004.
30. **Willey CD, Palanisamy AP, Johnston RK, Mani SK, Shiraishi H, Tuxworth WJ, Zile MR, Balasubramanian S, Kuppuswamy D.** STAT3 activation in pressure-overloaded feline myocardium: role for integrins and the tyrosine kinase BMX. *Int J Biol Sci* 4: 184–199, 2008.
31. **Xuan YT, Guo Y, Han H, Zhu Y, Bolli R.** An essential role of the JAK-STAT pathway in ischemic preconditioning. *Proc Natl Acad Sci USA* 98: 9050–9055, 2001.
32. **Zhang J, Ping P, Wang GW, Lu M, Pantaleon D, Tang XL, Bolli R, Vondriska TM.** Bmx, a member of the Tec family of nonreceptor tyrosine kinases, is a novel participant in pharmacological cardioprotection. *Am J Physiol Heart Circ Physiol* 287: H2364–H2366, 2004.
33. **Zhang YM, Bo J, Taffet GE, Chang J, Shi J, Reddy AK, Michael LH, Schneider MD, Entman ML, Schwartz RJ, Wei L.** Targeted deletion of ROCK1 protects the heart against pressure overload by inhibiting reactive fibrosis. *FASEB J* 20: 916–925, 2006.
34. **zur Nedden S, Tomaselli B, Baier-Bitterlich G.** HIF-1 alpha is an essential effector for purine nucleoside-mediated neuroprotection against hypoxia in PC12 cells and primary cerebellar granule neurons. *J Neurochem* 105: 1901–1914, 2008.

Immunology Letters 127 (2010) 135–142

Contents lists available at ScienceDirect

Immunology Letters

journal homepage: www.elsevier.com/locate/

Tec protein tyrosine kinase inhibits CD25 expression in human T-lymphocyte

Kentaro Susaki[a], Akira Kitanaka[b], Hiroaki Dobashi[a,*], Yoshitsugu Kubota[c], Katsuharu Kittaka[a], Tomohiro Kameda[a], Genji Yamaoka[b], Hiroyuki Mano[d], Keichiro Mihara[e], Toshihiko Ishida[a]

[a] Division of Endocrinology and Metabolism, Hematology, Rheumatology, and Respiratory Medicine, Department of Internal Medicine, Faculty of Medicine, Kagawa University, 1750-1 Ikenobe, Miki-cho, Kita-gun, Kagawa 761-0793, Japan
[b] Department of Laboratory Medicine, Faculty of Medicine, Kagawa University, 1750-1 Ikenobe, Miki-cho, Kita-gun, Kagawa 761-0793, Japan
[c] Department of Transfusion Medicine, Faculty of Medicine, Kagawa University, 1750-1 Ikenobe, Miki-cho, Kita-gun, Kagawa 761-0793, Japan
[d] Division of Functional Genomics, Jichi Medical University, 3311-1 Yakushiji, Shimotsuke-shi, Tochigi 329-0498, Japan
[e] Department of Hematology and Oncology, Research Institute for Radiation Biology and Medicine, Hiroshima University, 1-2-3 Kasumi, Minami-ku, Hiroshima 734-8553, Japan

ARTICLE INFO

Article history:
Received 16 July 2009
Received in revised form 21 October 2009
Accepted 23 October 2009
Available online 31 October 2009

Keywords:
Tec
CD25
T-lymphocyte

ABSTRACT

The Tec protein tyrosine kinase (PTK) belongs to a group of structurally related nonreceptor PTKs that also includes Btk, Itk, Rlk, and Bmx. Previous studies have suggested that these kinases play important roles in hematopoiesis and in the lymphocyte signaling pathway. Despite evidence suggesting the involvement of Tec in the T-lymphocyte activation pathway via T-cell receptor (TCR) and CD28, Tec's role in T-lymphocytes remains unclear because of the lack of apparent defects in T-lymphocyte function in Tec-deficient mice. In this study, we investigated the role of Tec in human T-lymphocyte using the Jurkat T-lymphoid cell line stably transfected with a cDNA encoding Tec. We found that the expression of wild-type Tec inhibited the expression of CD25 induced by TCR cross-linking. Second, we observed that LFM-A13, a selective inhibitor of Tec family PTK, rescued the suppression of TCR-induced CD25 expression observed in wild-type Tec-expressing Jurkat cells. In addition, expression of kinase-deleted Tec did not alter the expression level of CD25 after TCR ligation. We conclude that Tec PTK mediates signals that negatively regulate CD25 expression induced by TCR cross-linking. This, in turn, implies that this PTK plays a role in the attenuation of IL-2 activity in human T-lymphocytes.

1. Introduction

The activation and development of lymphocytes are regulated by the engagement of cell surface immune cell antigen receptors. Following receptor engagement, these receptors transmit signals by the activation of cytoplasmic protein tyrosine kinases (PTKs), such as Src, Syk, and Tec families [1,2]. The Tec family PTKs are nonreceptor PTKs including Tec, Btk, Itk (Emt/Tsk), Rlk (Txk), and Bmx (Etk). They are typically characterized by a pleckstrin-homology domain, a Tec-homology domain, Src homology domains (SH2 and SH3), and a kinase domain [3,4]. The biological importance of the Tec PTK subfamily was first confirmed in B-lymphocytes by the finding that Btk is essential for B-cell development [5,6] and that mutations in Btk cause X-linked agammaglobulinemia (XLA) in humans and B-cell defects in *xid* mice [7–10]. For T-cells, mice lacking Itk exhibited decreased numbers of mature thymocytes and reduced proliferative responses to both allogeneic major histocompatibility complex stimulation and T-cell receptor (TCR) cross-linking [11]. In addition, TCR-induced phosphorylation and activation of PLC-γ are reduced in T-cells lacking Itk [12]. According to early observations, it has been speculated that the functions of Btk and Itk are essentially related to B- and T-lymphoid development and activation, respectively, while Tec participates mainly in signaling pathways regulating myeloid cell growth and differentiation.

In our previous studies, we revealed Tec's contribution to antigen receptor signaling in B-lymphoid cells. Ligation of the B-cell receptor (BCR), CD19, and CD38 caused tyrosine phosphorylation of Tec and increased Tec PTK activity [13]. Tec's important role in B-cells was further confirmed by the generation of Tec/Btk double-deficient mice exhibiting an early block in B-cell development and a severe reduction in peripheral B-cell numbers [14]. In T-cells, TCR stimulation induces the activation of Itk [15], Rlk [16], and Tec [17]. In addition, the ligation of T-cell costimulatory receptor CD28 also activates Itk [18] and Tec [17]. In primary splenocytes from 5C.C7 TCR-transgenic mice, depletion of Tec using an antisense oligonucleotide treatment reduces IL-2 production in response to TCR ligation [19]. Studies using the Tec-transfected Jurkat human T-lymphoid cell line proposed the unique roles of Tec in T-cell activation [17,20]. However, purified T-cells from Tec-deficient mice were reported to have no apparent defects in TCR or CD28 signaling [14]. Thus, it is still an open question whether or not Tec is essential in the signaling pathway of T-lymphoid cells.

* Corresponding author. Tel.: +81 87 891 2145; fax: +81 87 891 2147.
E-mail address: hdobashi@med.kagawa-u.ac.jp (H. Dobashi).

0165-2478/$ – see front matter © 2009 Elsevier B.V. All rights reserved.
doi:10.1016/j.imlet.2009.10.009

In the present study we investigated Tec's role in human T-lymphoid cells using a Jurkat cell line stably transfected with a cDNA encoding Tec. We found that the expression of wild-type Tec inhibited the expression of CD25 induced by TCR cross-linking. Second, we observed that LFM-A13, a selective inhibitor of Tec family PTK, rescued the suppression of TCR-induced CD25 expression observed in wild-type Tec-expressing Jurkat cells. In addition, expression of kinase-deleted Tec did not alter the CD25 expression level after TCR ligation. We conclude that Tec PTK activity mediates signals that negatively regulate CD25 expression induced by TCR cross-linking in human T-lymphocytes.

2. Materials and methods

2.1. Reagents and cells

The rabbit polyclonal anti-Tec antibodies were previously described [13]. A monoclonal antibody to phosphotyrosine (PY99) and goat antisera to Tec were purchased from Santa Cruz Biotechnology (Santa Cruz, CA). Monoclonal anti-CD3 antibody (OKT3) was obtained from Janssen Pharmaceutical (Tokyo, Japan). Monoclonal anti-CD28 antibody was from Immunotech (Marseille, France). PE-conjugated anti-CD25 antibody and FITC-conjugated anti-CD69 antibody were from Dako (Glostrup, Denmark). LFM-A13 (a-cyano-b-hydroxy-b-methyl-N-(2,5-dibromophenyl) propenamide) was from Calbiochem (San Diego, CA). LFM-A13 was dissolved in dimethyl sulfoxide (DMSO) and aliquots were stored at −30 °C. The final concentration of DMSO was less than 0.5% for all experiments. DMSO at this concentration had no discernible effect on cell growth or surface marker expression profiles, including CD3 and CD25 expression (data not shown). All other agents were purchased from commercial sources.

The Jurkat human T-lymphoid cell line was a generous gift from Dr. D. Campana (St. Jude Children's Research Hospital, Memphis, TN). Jurkat cells were maintained in RPMI-1640 (Sigma, St. Louis, MO) with 10% fetal calf serum, L-glutamine, and antibiotics.

2.2. Immunoprecipitation, electrophoresis, and Western blotting

The cells were lysed in lysis buffer (50 mM Tris–HCl [pH 7.5], 150 mM NaCl, 1% [v/v] Triton X-100, 1 mM Na_3VO_4, 1 mM phenylmethyl-sulfonyl fluoride, 5 μg/ml aprotinin, 1 mM EDTA–2Na). Immunoprecipitation and Western blotting analysis were performed as described previously [13]. The experiments were repeated independently at least three times.

2.3. DNA constructs and electroporation conditions

The construction of pSR expression vector containing cDNA of wild-type Tec (TecWT) and kinase-deleted Tec (TecKD) has been described elsewhere [21]. Jurkat cells (5×10^6/experiment) were subjected to electroporation with 30 μg of pSR or pSR containing TecWT or TecKD, as described previously [22]. Transfected cells were selected after 2 weeks' culture in the presence of 5 μg/ml of blasticidin S hydrochloride (Funakoshi, Tokyo, Japan). Blasticidin-resistant clones were expanded and screened for Tec expression by means of immunoprecipitation and Western blotting. Individual clones were cultured and were analyzed as a mixture of clones to avoid clonal variations.

2.4. Stimulation of T cells

Anti-CD3 antibody (2 μg/ml) was incubated in 24-well flat-bottom plates at 4 °C for 16 h for immobilization to the bottoms of the plates. The plates were washed twice to remove excess antibodies. Cells were incubated in each well of anti-CD3-coated plates at 37 °C in 5% CO_2 with 90% humidity for indicated periods. At the termination of the cultures, the cells were harvested, suspended in PBS, and subjected to further analysis. The experiments were repeated independently at least three times.

2.5. Flow cytometric analysis

The surface phenotypes of the cells were examined by flow cytometry as described previously [23]. Briefly, collected cells were incubated with a specific fluorescent-conjugated monoclonal antibody or control mouse IgG on ice for 30 min. After two washes with PBS, cells were analyzed with an EPICS XL flow cytometry system equipped with EXPO32 ADC software (Beckman Coulter, Miami, FL). The experiments were repeated independently three times.

2.6. Quantification of IL-2

To measure IL-2 production, Jurkat cells were cultured in 24-well plates at 1×10^6 cells/ml, 1 ml/well and stimulated with 2 μg/ml anti-CD3 plus 2 μg/ml anti-CD28 monoclonal antibodies, or 50 ng/ml PMA and 1 μM ionomycin for the positive control cultures. After 24 h culture, IL-2 secreted in the culture supernatant was measured using Quantiflow Human IL-2 Immunoassay kits (BioE, St. Paul, MN) according to the manufacturer's instructions. The experiments were repeated independently at least three times.

2.7. RT-PCR analysis

RT-PCR analysis was performed as described previously [24]. For amplification of the cDNA products, the following oligodeoxynucleotide primers were used: CD25 primers, 5′-GGGATACAGGGCTCTACACAG-3′ (sense) and 5′-ACCTGGAAACTGACTGGTCTC-3′ (antisense); β-actin primers, 5′-ATCATGTTTGAGACCTTCAA-3′ (sense) and 5′-GATGTCCACGTCACACTTCA-3′ (antisense). The PCR product was resolved by agarose gel electrophoresis and analyzed by means of densitometric analysis, and the fold increase in the CD25 cDNA level was normalized to the β-actin product. The experiments were repeated independently at least three times.

2.8. Statistical analysis

Data were analyzed by Student's *t*-test; $P < 0.05$ was considered to indicate a statistically significant difference.

3. Results

3.1. Ectopic expression and activation of Tec in Jurkat cells

As we reported previously, Jurkat cells lack endogenous Tec expression [13,25], making this cell line a useful model for studying the role of Tec in human T-cell biology. To investigate the role of Tec in human T-lymphoid cells, we introduced Tec cDNA to Jurkat cells. Clonal Jurkat cells expressing Tec protein (Jurkat-TecWT cells) were obtained after transfection and a subsequent series of limiting dilution procedures (Fig. 1a). In contrast, proteins in the anti-Tec immunoprecipitates from mock-transfected Jurkat cells (Jurkat-Mock cells) did not react with anti-Tec antibody (Fig. 1a). Ligation of TCR or CD28 is known to induce tyrosine phosphorylation of intracellular proteins in T-lymphoid cells, including Jurkat cell lines [1]. To determine whether or not the signaling pathways triggered by TCR or CD28 ligation were affected by the presence of Tec, intracellular protein tyrosine phosphorylation was analyzed by Western blotting using anti-phosphotyrosine antibody. As shown in Fig. 1b, in Jurkat-TecWT cells the ligation of CD3 or CD28 induced tyrosine phosphorylation with molecular weights and intensities

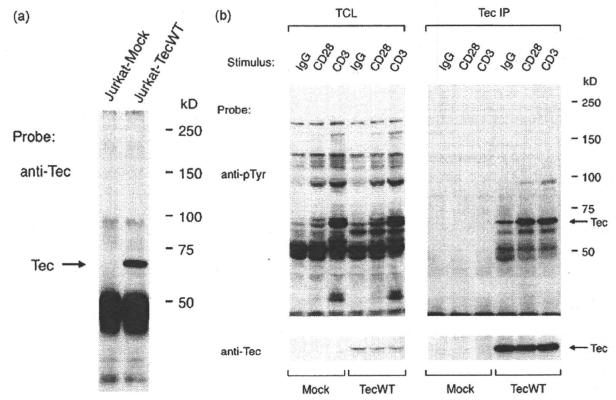

Fig. 1. Ectopically expressed Tec is activated following cell surface receptor cross-linking in Jurkat cells. (a) Cell lysates of Jurkat-Mock cells and Jurkat-TecWT cells were subjected to immunoprecipitation with anti-Tec antibody. Proteins were separated by SDS-PAGE and transferred to a PVDF membrane. The membrane was probed with anti-Tec polyclonal antibody. The positions of Tec and molecular mass markers (in kDa) are indicated. The intense band of approximately 50 kDa corresponds to the Ig heavy chain of the antibody used for immunoprecipitation. (b) Jurkat-Mock cells and Jurkat-TecWT cells were stimulated with control IgG, anti-CD28, or anti-CD3 for 5 min. Total cell lysates (TCLs) and proteins immunoprecipitated with anti-Tec (Tec IP) from these lysates were separated by SDS-PAGE and transferred to a PVDF membrane. The membrane was probed with anti-phosphotyrosine antibody (anti-pTyr; upper panel), then stripped and reprobed with anti-Tec polyclonal antibody (lower panel). The positions of Tec and molecular mass markers (in kDa) are indicated.

similar to those seen in Jurkat-Mock cells. Thus, the ectopic expression of Tec did not affect the overall profile and magnitude of the tyrosine-phosphorylated proteins, at least to an extent detectable by Western blotting. To determine whether or not TCR signaling activated transfected Tec in Jurkat cells, we examined Tec tyrosine phosphorylation after cross-linking the TCR with an anti-CD3 antibody. In contrast to the lack of a significant effect of Tec expression on the overall pattern of tyrosine phosphorylation, exposure to anti-CD3 antibody markedly increased tyrosine phosphorylation of Tec in Jurkat-TecWT cells (Fig. 1b). Stimulation of cells with anti-CD28 also triggered the tyrosine phosphorylation of Tec. Thus, activation of transfected Tec by ligation of T-cell-specific surface molecules was confirmed in Jurkat-TecWT cells. No tyrosine phosphorylation signal was detected in anti-Tec immunoprecipitates obtained from Jurkat-Mock cells (Fig. 1b).

We next examined the effect of Tec expression on Jurkat cell surface marker expression. The cell surface antigenic phenotype of Jurkat-TecWT cells was investigated by flow cytometry and compared with that of Jurkat-Mock cells. No apparent differences were observed in the expression of T-lymphoid cell markers and the activation markers examined, such as, CD1, CD2, CD3, CD4, CD8, CD25, CD28, and CD69, indicating that Tec expression had a minimal effect on the basal expression of representative T-cell surface proteins (data not shown).

3.2. Effect of Tec on IL-2 production

Because Tec overexpression in Jurkat cells has been reported to enhance IL-2 production and can induce TCR-mediated phospholipase Cγ (PLC-γ) phosphorylation and NFAT (nuclear factor of activated T-cells) activation [17,19,20,26,27], we attempted to replicate those findings with Jurkat cells stably transfected with Tec. Unexpectedly, exposure of Jurkat-TecWT cells to anti-CD3 plus anti-CD28 resulted in low levels of IL-2 production in both Jurkat-Mock cells and Jurkat-TecWT cells, without significant differences between the two cell types. In one experiment, after 24 h of incubation, 36 pg/ml IL-2 with anti-CD3 plus anti-CD28 stimulation versus 845 pg/ml IL-2 in control cultures with 50 ng/ml of PMA and 1 μM ionomycin were detected in the supernatant of the Jurkat-Mock cell culture, while 10 pg/ml IL-2 versus 850 pg/ml IL-2 was detected in the Jurkat-TecWT cell culture. Low IL-2 secretion in response to TCR stimulation was reproduced in both cell lines in repeated experiments. The addition of IL-2 at concentrations below 100 pg/ml had no influence on CD25 expression in either Jurkat-Mock cells or Jurkat-TecWT cells (data not shown).

3.3. Tec downregulates CD25 expression

CD25 is an essential component of high-affinity IL-2 receptors [28,29]. Although several investigators have proposed the possibility that Tec is involved in the IL-2-producing machinery [4,17,19,20,26,27,31,32,35], little is known about the relationship between Tec family PTK and CD25 expression, except the downregulation of CD25 observed in stimulated T-cells from Itk-deficient mice [12]. We evaluated the effect of Tec expression in Jurkat cells on CD25 expression. The membrane expression of CD25 increases after T-lymphocyte activation [28,29]. To examine whether or not Tec expression modifies TCR-mediated signaling, we examined changes in CD25 surface expression on Jurkat-derived clones activated for 24 h with TCR cross-linking using flow cytometry. As shown in Fig. 2a , enhanced CD25 expression was observed in Jurkat-Mock cells after the 24 h incubation with plate-bound anti-CD3. In contrast, the expression of CD25 after TCR cross-linking was markedly suppressed in Jurkat-TecWT cells (Fig. 2a). The percentage of CD25-expressing cells after TCR cross-linking was 39.5% in Jurkat-Mock cells and 9.9% in Jurkat-TecWT cells. These findings suggest that activation of Tec kinase results in the downregulation of CD25 expression induced by TCR cross-linking. CD69 (an activation-inducer molecule) is also known to be upregulated upon T-cell activation [1,12]. Next, we examined the effect

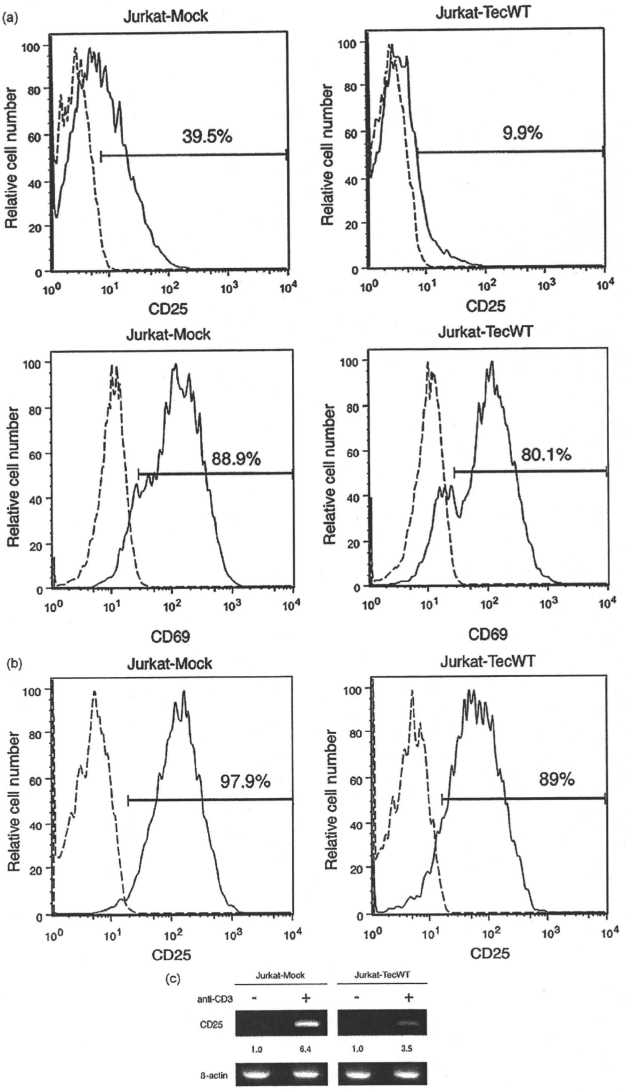

Fig. 2. Expression of Tec inhibits upregulation of CD25 but not that of CD69 induced by TCR cross-linking. (a) Jurkat-Mock cells and Jurkat-TecWT cells after TCR cross-linking were incubated with anti-CD25 (upper panels) and anti-CD69 (lower panels) antibodies. Flow cytometric histograms show the intensity of staining with the indicated antibody (solid line) compared with that of an isotype-matched nonreactive control antibody (broken line). (b) Jurkat-Mock cells and Jurkat-TecWT cells cultured

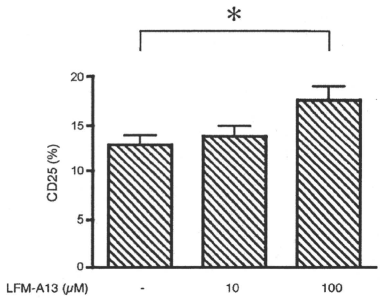

Fig. 3. Tec selective inhibitor LFM-A13 increases the CD25 expression on Jurkat-TecWT cells after TCR cross-linking. Jurkat-TecWT cells were treated with the indicated concentrations of LFM-A13 or DMSO (vehicle) for 1 h. The cells were then stimulated with TCR cross-linking for 24 h. CD25 expression was evaluated by means of flow cytometric analysis. Bars (mean ± SD of quadruplicate tests) represent the percentage of cells expressing CD25. *$P < 0.05$.

of Tec expression on the induction of CD69 caused by TCR cross-linking. Although CD25 expression was markedly suppressed after TCR stimulation in Jurkat-TecWT cells, no apparent difference was observed on the CD69 expression between Jurkat-Mock cells and Jurkat-TecWT cells (Fig. 2a). Thus, Tec expression inhibited CD25 expression after TCR cross-linking, without affecting CD69 induction. The defect in the signal seems to be adjacent to TCR, as Tec expression does not affect the CD25 expression level in Jurkat cells after PMA plus ionomycin activation, which bypasses the early stage signals induced by TCR cross-linking (Fig. 2b).

CD25 gene expression is tightly regulated at the transcriptional level [28,29]. Therefore, we next investigated the expression of CD25 mRNA in Jurkat-derived clones. Using RT-PCR, we examined the effect of TCR cross-linking on CD25 mRNA expression in Jurkat clones. As shown in Fig. 2c, CD25 mRNA expression in Jurkat-Mock cells was increased after 24 h stimulation with TCR cross-linking. In contrast, the increase in CD25 mRNA expression in Jurkat-TecWT cells after TCR cross-linking was markedly suppressed. The densitometric analysis of the relative intensities (means ± S.E.) of three independent experiments showed significant inhibition of the CD25 mRNA expression in Jurkat-TecWT cells after TCR cross-linking ($P < 0.05$) (data not shown). These results imply the importance of Tec PTK on the downregulation of CD25 expression after TCR cross-linking.

To further elucidate the contribution of Tec PTK activity on the results obtained by comparing Jurkat clones with or without Tec, we took advantage of LFM-A13, a compound that preferentially inhibits the enzymatic activity of Tec family PTKs both *in vitro* and *in vivo* [30] in order to investigate Tec's role in the regulation of CD25 expression. We examined LFM-A13's effect on CD25 surface expression in Jurkat-TecWT cells after TCR cross-linking. LFM-A13 dose-dependently increased CD25 expression in Jurkat-TecWT cells after TCR cross-linking (Fig. 3). After 24 h of culture, 17.6 ± 2.8% of cells incubated with 100 μM LFM-A13 expressed CD25, versus 12.9 ± 2.1% of cells in control cultures. CD3 surface expression was not altered when measured after 1 or 24 h incubation of Jurkat-TecWT cells with LFM-A13 (data not shown). Thus, LFM-A13's effect was not due to the modulation of cell-surface CD3 expression. In Jurkat-Mock cells, CD25 surface expression induced by TCR cross-linking was not affected by the presence of LFM-A13 (data not shown).

To corroborate the results obtained using LFM-A13, we established stable transfectants of Jurkat cells expressing a kinase domain-deleted Tec (Jurkat-TecKD) (Fig. 4a). Although rapid and transient tyrosine phosphorylation of Tec was observed after ligation of TCR in Jurkat-TecWT cells, no detectable tyrosine phosphorylation was observed in TecKD protein obtained from Jurkat-TecKD cells throughout the time course examined (Fig. 4b). In Jurkat-TecKD cells, CD25 expression after TCR cross-linking was comparable to that of Jurkat-Mock cells (Fig. 4c and d). These results indicate that Tec PTK activity contributes to the downregulation of CD25 observed in TCR-stimulated Jurkat-TecWT cells.

4. Discussion

Studies of Tec family PTKs have begun to reveal the crucial roles of these kinases in transducing stimuli triggered by immune cell antigen receptors, such as TCR and BCR, regulating lymphoid cell development and activation [31,32]. Targeted disruption of Tec family PTK genes has revealed the unique roles of individual PTKs in lymphocyte signal transduction. In T-cells, Itk and Rlk play important roles in the TCR-mediated signaling pathway, which leads to the phosphorylation and activation of PLC-γ, an essential step in lymphoid cell activation [4,33–35]. Despite evidence suggesting Tec's involvement in TCR and CD28 signaling, Tec's role in T-lymphocyte remains unclear because of the lack of an overt defect in T-lymphocyte function in Tec-deficient mice [14]. Recent findings indicating that Itk and Rlk have nonessential roles in pre-TCR signaling in the thymus [36] may suggest that Tec has a compensatory effect on the lack of these kinases in T-cell development. In the present study, we attempted to address Tec's role in human T-lymphocyte function using Jurkat cells stably transfected with Tec-based constructs. We have demonstrated that Tec PTK activation results in the suppression of TCR-induced CD25 expression, implying that this PTK transmits signals attenuating IL-2 activity in human T-lymphocytes.

IL-2 transmits its effects via a high-affinity IL-2 receptor, which is composed of three transmembrane proteins (α, β, γc subunits) [28,29]. The binding of CD25 (α subunit) to the low-affinity IL-2R (β, γc subunits) increases affinity to IL-2, enhancing the cellular responses to the low concentration of IL-2. A very small population of circulating mononuclear cells expresses CD25 in normal human peripheral blood. After antigen-induced activation, CD25 was strongly expressed in human T-lymphocytes [28,29]. CD25 expression is induced not only by antigen-induced activation, but also by various mitogenic stimulations including cytokines such as IL-1, IL-2, IL-7, IL-12, IL-15, IL-16, TNF-α, TGF-β, and IFN-α [28,29]. There have been extensive studies of how CD25 expression is regulated in response to these stimuli. CD25 expression is believed to be controlled mostly at the stage of transcription regulation. Therefore, the promoter lesions of CD25 have been analyzed in detail, and multiple molecules regulating its transcriptional level have been identified [28,29]. In contrast, relatively little effort has been made to identify the PTK that plays a key role in CD25 expression after T-cell activation. Although a higher degree of CD25 upreg-

with 50 ng/ml of PMA and 1 μM ionomycin were incubated with anti-CD25 antibody. Flow cytometric histograms show the intensity of staining with anti-CD25 antibody (solid line) compared with that of an isotype-matched nonreactive control antibody (broken line). (c) Total RNA was isolated from Jurkat-Mock cells and Jurkat-TecWT cells with or without TCR cross-linking using anti-CD3 antibody. The expression of CD25 mRNA in the cells was analyzed by means of RT-PCR using specific primers as described in Section 2. The expression of β-actin was used as a control. The intensity of the CD25 mRNA band was measured by scanning densitometry and normalized to β-actin. The fold change in CD25 mRNA after TCR cross-linking is shown in comparison with the level in the unstimulated cells as the average of three independent experiments.

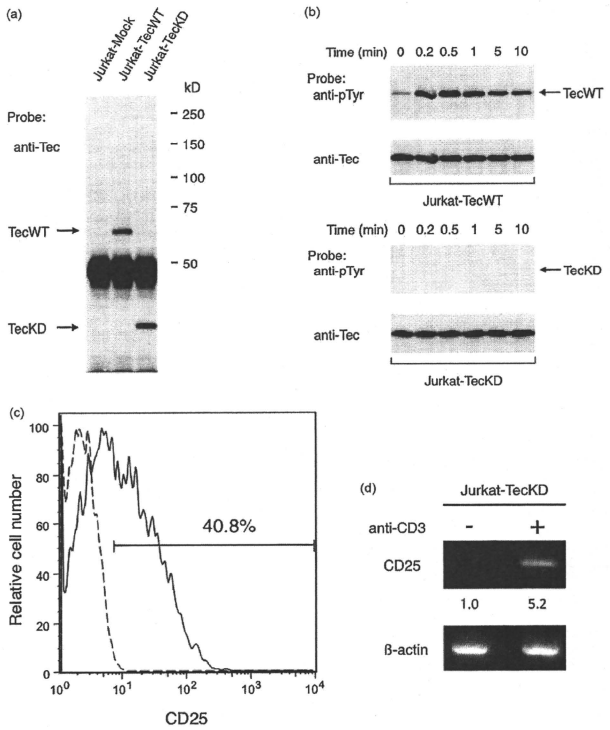

Fig. 4. Expression of Tec that lacks a kinase domain does not alter CD25 expression induced by TCR cross-linking. (a) Cell lysates of Jurkat-Mock cells, Jurkat-TecWT cells, and Jurkat-TecKD cells were subjected to immunoprecipitation with anti-Tec antibody and analyzed by Western blotting using anti-Tec antibody. The positions of TecWT and TecKD and molecular mass markers (in kDa) are indicated. The intense band of approximately 50 kDa corresponds to the Ig heavy chain of the antibody used for immunoprecipitation. (b) Jurkat-TecWT cells and Jurkat-TecKD cells were incubated with anti-CD3 antibody for the times indicated. Cell lysates were prepared and subjected to immunoprecipitation with anti-Tec antibody. The membrane was probed with anti-phosphotyrosine antibody (anti-pTyr; upper panel), then stripped and reprobed with anti-Tec polyclonal antibody (lower panel). The positions of TecWT and TecKD are indicated. (c) Jurkat-TecKD cells after TCR cross-linking were incubated with anti-CD25 antibody (solid line) or nonreactive control antibody (broken line), both conjugated to PE, and the fluorescence intensity was analyzed by flow cytometry. (d) Total RNA was isolated from Jurkat-TecKD cells with or without TCR cross-linking. The expression of CD25 mRNA in the cells was analyzed by means of RT-PCR using specific primers as described in Section 2. The expression of β-actin was used as a control. The intensity of the CD25 mRNA band was measured by scanning densitometry and normalized to β-actin. The fold change in CD25 mRNA after TCR cross-linking is shown in comparison with the level in the unstimulated cells as the average of three independent experiments.

ulation on wild-type T-cells compared with Itk-deficient T-cells was observed after TCR cross-linking, this difference is attributed to the IL-2-induced increase in CD25 expression, which is absent in Itk-deficient T-cells [12]. In our Jurkat system, the effect of Tec expression on IL-2 production was too small to alter CD25 expression level. The inefficient expression of CD25 in Jurkat-TecWT cells upon TCR stimulation seems to be dependent on the Tec PTK activity. Thus, the induction and activation of Tec in TCR-stimulated T-cells may impair the regulation of CD25 expression, resulting in the attenuation of IL-2-induced biological effects accomplished by autocrine and paracrine mechanisms. Prolonged upregulation of Tec relative to that of Itk in primary T-cells following anti-CD3 plus anti-CD28 stimulation [20] may imply that Tec has a negative regulatory role in the latter phase of the TCR-mediated signaling pathway. In human CD4+ T-cells, the Tec expression 24 h after TCR cross-linking was not altered (Susaki and Kitanaka, unpublished observation). Due to the difficulty of maintaining cell viability after sustained cell culture, we failed to examine the Tec expression level within the long time course in TCR-stimulated human CD4+ T-cells.

Previous studies using Jurkat cells have revealed that Tec overexpression enhances IL-2 promoter activity [17,19,26,27]. In our study, IL-2 production did not differ significantly between Jurkat-TecWT cells and Jurkat-Mock cells after anti-CD3 plus anti-CD28 stimulation. There is an apparent discrepancy between our find-

ings and those of previous studies. This may simply reflect clonal variations of individual Jurkat cell lines maintained in individual laboratories. Another possible explanation for the conflicting results is that these studies employed different gene transfer methods. Our experiment was performed using Jurkat cells stably transfected with Tec cDNA, whereas others carried out experiments with Jurkat cells transiently transfected with Tec. In most of the experimental conditions, transient transfection of cDNA results in higher levels of protein expression than those observed in the stable transformants. The differences in Tec expression levels among the experiments may have had diverse cellular effects.

In Epstein-Barr virus (EBV)-transformed B-lymphoblastoid cell lines from XLA patients, Fluckiger et al. [37] showed that the ectopic expression not only of Btk but also of Tec or Itk restored deficient extracellular calcium influx after BCR cross-linking in Btk-deficient cells. We, as well as Fluckiger et al. [13,37], have found that these XLA-derived Btk-deficient cell lines express endogenous Tec. The difference in the expressed amount of protein is considered the cause of the endogenous Tec's inability to compensate for Btk deficiencies. Interestingly, the overexpression of other PTK family members, such as Src (Lyn or Fyn) and Syk, failed to restore Btk-mediated signaling in XLA cells, suggesting the presence of strict kinase-substrate relationships between different PTK families regardless of the expression level [37]. These observations suggest that the expression of excess amounts of proteins may overcome the substrate specificity among individual Tec family PTKs that are present under physiological protein expression levels. This hypothesis is supported by our failure to detect any alteration of CD25 expression after TCR ligation in human primary CD4+ T-cells transiently transfected with Tec cDNA (Susaki and Kitanaka, unpublished observation). To reproduce findings obtained using the Jurkat cell line in human primary T-cells, it may be essential to establish a more sophisticated method to regulate the expression of introduced genes.

Tomlinson et al. [20] quantitated individual Tec family PTK protein levels in murine lymphoid cells. They found substantially lower Tec expression in murine primary T- and B-cells relative to Itk and Btk, respectively. They speculated that the lack of an obvious phenotype in the immune systems of Tec-deficient mice reflected the small amounts of Tec in murine lymphoid cells. Although there is not enough quantitative information on Tec expression relative to other Tec family PTKs in human lymphoid cells, our previous study revealed that EBV-transformed human B-lymphoblastoid cell lines expressed Tec levels similar to those observed in the K562 human erythroleukemia cell line [13]. In this regard, it is clear that human B-lymphoid cells express an amount of Tec comparable to the amounts in the representative human myeloid cell line. Therefore, the inability of a physiological amount of Tec to compensate for Btk in human lymphoid cells may be the reason why defective Btk function results in more severe consequences in humans than in mice [14,38]. Thus, the expression profiles and/or functional redundancies of individual Tec family PTK in lymphoid cells may differ among species. To clarify this issue, the Tec expression level should be compared against Tec's biological significance in human lymphoid cells. It is necessary to assess Tec expression in human lymphoid cells at different stages of development using quantitative methods such as flow cytometric analysis. To date, such analysis has not yet been accomplished because of the lack of a good anti-Tec antibody applicable to flow cytometric analysis (Kitanaka, unpublished observations).

In summary, we have found that the expression and activation of Tec in Jurkat cells inhibited the expression of CD25 induced by TCR cross-linking, suggesting that this PTK plays a negative regulatory role in the TCR-mediated signaling pathway. Our results imply that Tec participates in signaling that suppresses IL-2-mediated signaling by downregulating its receptor expression. Future studies should clarify the role of Tec expression and activation in the IL-2/IL-2 receptor system-mediated human T-lymphocyte activation pathway.

Acknowledgment

We thank K. Sangawa for her excellent technical assistance.

References

[1] Kane LP, Lin J, Weiss A. Signal transduction by the TCR for antigen. Curr Opin Immunol 2000;12:242–9.
[2] Wang LD, Clark MR. B-cell antigen-receptor signalling in lymphocyte development. Immunology 2003;110:411–20.
[3] Kawakami Y, Yao L, Han W, Kawakami T. Tec family protein-tyrosine kinases and pleckstrin homology domains in mast cells. Immunol Lett 1996;54:113–7.
[4] Miller AT, Berg LJ. New insights into the regulation and functions of Tec family tyrosine kinases in the immune system. Curr Opin Immunol 2002;14:331–40.
[5] Khan WN, Alt FW, Gerstein RM, Malynn BA, Larsson I, Rathbun G, et al. Defective B cell development and function in Btk-deficient mice. Immunity 1995;3:283–99.
[6] Kerner JD, Appleby MW, Mohr RN, Chien S, Rawlings DJ, Maliszewski CR, et al. Impaired expansion of mouse B cell progenitors lacking Btk. Immunity 1995;3:301–12.
[7] Vetrie D, Vorechovský I, Sideras P, Holland J, Davies A, Flinter F, et al. The gene involved in X-linked agammaglobulinaemia is a member of the src family of protein-tyrosine kinases. Nature 1993;361:226–33.
[8] Tsukada S, Saffran DC, Rawlings DJ, Parolini O, Allen RC, Klisak I, et al. Deficient expression of a B cell cytoplasmic tyrosine kinase in human X-linked agammaglobulinemia. Cell 1993;72:279–90.
[9] Thomas JD, Sideras P, Smith CIE, Vorechovsky I, Chapman V, Paul WE. Colocalization of X-linked agammaglobulinemia and X-linked immunodeficiency genes. Science 1993;261:355–8.
[10] Rawlings DJ, Saffran DC, Tsukada S, Largaespada DA, Grimaldi JC, Cohen L, et al. Mutation of unique region of Bruton's tyrosine kinase in immunodeficient XID mice. Science 1993;261:358–61.
[11] Liao XC, Littman DR. Altered T cell receptor signaling and disrupted T cell development in mice lacking Itk. Immunity 1995;3:757–69.
[12] Liu KQ, Bunnell SC, Gurniak CB, Berg LJ. T cell receptor-initiated calcium release is uncoupled from capacitative calcium entry in Itk-deficient T cells. J Exp Med 1998;187:1721–7.
[13] Kitanaka A, Mano H, Conley ME, Campana D. Expression and activation of the nonreceptor tyrosine kinase Tec in human B cells. Blood 1998;91:940–8.
[14] Ellmeier W, Jung S, Sunshine MJ, Hatam F, Xu Y, Baltimore D, et al. Severe B cell deficiency in mice lacking the tec kinase family members Tec and Btk. J Exp Med 2000;192:1611–24.
[15] Tanaka N, Abe H, Yagita H, Okumura K, Nakamura M, Sugamura K. Itk, a T cell-specific tyrosine kinase, is required for CD2-mediated interleukin-2 promoter activation in the human T cell line Jurkat. Eur J Immunol 1997;27:834–41.
[16] Debnath J, Chamorro M, Czar MJ, Schaeffer EM, Lenardo MJ, Varmus HE, et al. rlk/TXK encodes two forms of a novel cysteine string tyrosine kinase activated by Src family kinases. Mol Cell Biol 1999;19:1498–507.
[17] Yang WC, Ghiotto M, Barbarat B, Olive D. The role of Tec protein-tyrosine kinase in T cell signaling. J Biol Chem 1999;274:607–17.
[18] August A, Gibson S, Kawakami Y, Kawakami T, Mills GB, Dupont B. CD28 is associated with and induces the immediate tyrosine phosphorylation and activation of the Tec family kinase ITK/EMT in the human Jurkat leukemic T-cell line. Proc Natl Acad Sci USA 1994;91:9347–51.
[19] Yang WC, Ching KA, Tsoukas CD, Berg LJ. Tec kinase signaling in T cells is regulated by phosphatidylinositol 3-kinase and the Tec pleckstrin homology domain. J Immunol 2001;166:387–95.
[20] Tomlinson MG, Kane LP, Su J, Kadlecek TA, Mollenauer MN, Weiss A. Expression and function of Tec, Itk, and Btk in lymphocytes: evidence for a unique role for Tec. Mol Cell Biol 2004;24:2455–66.
[21] Yamashita Y, Watanabe S, Miyazato A, Ohya K, Ikeda U, Shimada K, et al. Tec and Jak2 kinases cooperate to mediate cytokine-driven activation of c-fos transcription. Blood 1998;91:1496–507.
[22] Kitanaka A, Suzuki T, Ito C, Nishigaki H, Coustan-Smith E, Tanaka T, et al. CD38-mediated signaling events in murine pro-B cells expressing human CD38 with or without its cytoplasmic domain. J Immunol 1999;162:1952–8.
[23] Dobashi H, Sato M, Tanaka T, Tokuda M, Ishida T. Growth hormone restores glucocorticoid-induced T cell suppression. FASEB J 2001;15:1861–3.
[24] Kubota Y, Tanaka T, Kitanaka A, Ohnishi H, Okutani Y, Waki M, et al. Src transduces erythropoietin-induced differentiation signals through phosphatidylinositol 3-kinase. EMBO J 2001;20:5666–77.
[25] Sato K, Mano H, Ariyama T, Inazawa J, Yazaki Y, Hirai H. Molecular cloning and analysis of the human Tec protein-tyrosine kinase. Leukemia 1994;8:1663–72.
[26] Yang WC, Ghiotto M, Castellano R, Collette Y, Auphan N, Nunès JA, et al. Role of Tec kinase in nuclear factor of activated T cells signaling. Int Immunol 2000;12:1547–52.
[27] Yang WC, Olive D. Tec kinase is involved in transcriptional regulation of IL-2 and IL-4 in the CD28 pathway. Eur J Immunol 1999;29:1842–9.

[28] Taniguchi T, Minami Y. The IL-2/IL-2 receptor system: a current overview. Cell 1993;73:5–8.
[29] Kim HP, Imbert J, Leonard WJ. Both integrated and differential regulation of components of the IL-2/IL-2 receptor system. Cytokine Growth Factor Rev 2006;17:349–66.
[30] Mahajan S, Ghosh S, Sudbeck EA, Zheng Y, Downs S, Hupke M, et al. Rational design and synthesis of a novel anti-leukemic agent targeting Bruton's tyrosine kinase (BTK), LFM-A13 [alpha-cyano-beta-hydroxy-beta-methyl-N-(2,5-dibromophenyl)propenamide]. J Biol Chem 1999;274:9587–99.
[31] Yang WC, Collette Y, Nunès JA, Olive D. Tec kinases: a family with multiple roles in immunity. Immunity 2000;12:373–82.
[32] Berg LJ, Finkelstein LD, Lucas JA, Schwartzberg PL. Tec family kinases in T lymphocyte development and function. Annu Rev Immunol 2005;23:549–600.
[33] Schaeffer EM, Debnath J, Yap G, McVicar D, Liao XC, Littman DR, et al. Requirement for Tec kinases Rlk and Itk in T cell receptor signaling and immunity. Science 1999;284:638–41.
[34] Kurosaki T. Regulation of B-cell signal transduction by adaptor proteins. Nat Rev Immunol 2002;2:354–63.
[35] Takesono A, Finkelstein LD, Schwartzberg PL. Beyond calcium: new signaling pathways for Tec family kinases. J Cell Sci 2002;115:3039–48.
[36] Lucas JA, Felices M, Evans JW, Berg LJ. Subtle defects in pre-TCR signaling in the absence of the Tec kinase Itk. J Immunol 2007;179:7561–7.
[37] Fluckiger AC, Li Z, Kato RM, Wahl MI, Ochs HD, Longnecker R, et al. Btk/Tec kinases regulate sustained increases in intracellular Ca^{2+} following B-cell receptor activation. EMBO J 1998;17:1973–85.
[38] Conley ME, Rohrer J, Rapalus L, Boylin EC, Minegishi Y. Defects in early B-cell development: comparing the consequences of abnormalities in pre-BCR signaling in the human and the mouse. Immunol Rev 2000;178:75–90.

Human Cancer Biology
See commentary p. 4909

Clinical Cancer Research

EML4-ALK Fusion Gene Assessment Using Metastatic Lymph Node Samples Obtained by Endobronchial Ultrasound-Guided Transbronchial Needle Aspiration

Yuichi Sakairi[1,7], Takahiro Nakajima[1,2,7], Kazuhiro Yasufuku[2], Dai Ikebe[3], Hajime Kageyama[4], Manabu Soda[5], Kengo Takeuchi[6], Makiko Itami[3], Toshihiko Iizasa[1], Ichiro Yoshino[7], Hiroyuki Mano[5], and Hideki Kimura[1]

Abstract

Purpose: Anaplastic lymphoma kinase (*ALK*) fusion genes represent novel oncogenes for non–small cell lung cancers (NSCLC). Several *ALK* inhibitors have been developed, and are now being evaluated in *ALK*-positive NSCLC. The feasibility of detecting *ALK* fusion genes in samples obtained by endobronchial ultrasound-guided transbronchial needle aspiration (EBUS-TBNA) was determined. The clinicopathologic characteristics of *ALK*-positive lung cancer were also analyzed.

Experimental Design: From April 2008 to July 2009, NSCLC cases with hilar/mediastinal lymph node metastases detected by EBUS-TBNA were enrolled. Positive expression of *ALK* fusion protein was determined using immunohistochemistry, and *ALK* gene rearrangements were further examined to verify the translocation between *ALK* and partner genes using fluorescent *in situ* hybridization and reverse transcription-PCR. Direct sequencing of PCR products was performed to identify *ALK* fusion variants.

Results: One hundred and nine cases were eligible for the analysis using re-sliced samples. Screening of these specimens with immunohistochemistry revealed *ALK* positivity in seven cases (6.4%), all of which possessed echinoderm microtubule–associated protein-like 4–*ALK* fusion genes as detected by fluorescent *in situ* hybridization and reverse transcription-PCR. All *ALK*-positive cases had an adenocarcinoma histology and possessed no *EGFR* mutations. Compared with *ALK*-negative cases, *ALK*-positive cases were more likely to have smaller primary tumors ($P < 0.05$), to occur at a younger age (<60 years; $P < 0.05$), and to occur in never/light smokers (smoking index < 400; $P < 0.01$). Mucin production was frequently observed in *ALK*-positive adenocarcinomas (29.4%; $P < 0.01$).

Conclusions: EBUS-TBNA is a practical and feasible method for obtaining tissue from mediastinal and hilar lymph nodes that can be subjected to multimodal analysis of *ALK* fusion genes in NSCLC.
Clin Cancer Res; 16(20); 4938–45. ©2010 AACR.

A small inversion within the short arm of human chromosome 2 leads to the generation of a fusion gene between the anaplastic lymphoma kinase (*ALK*) gene and the echinoderm microtubule–associated protein-like 4 (*EML4*) gene, the protein product of which is reported to function as an oncokinase in non–small cell lung cancer (NSCLC); in fact, this was the first oncogenic translocation to be identified in lung cancer (1). The *EML4-ALK* fusion gene has been detected in ~5% of NSCLC cases, and several *ALK* fusion gene variants have been reported (2). Standard methods for the detection of *ALK* fusion genes include reverse transcription-PCR (RT-PCR) with primers flanking the fusion points, as well as fluorescent *in situ* hybridization (FISH). Previously, immunohistochemistry-based diagnosis of *ALK* fusion genes in lung cancer has proven to be difficult, most likely due to the low expression level of the fusion protein products (3). An intercalated antibody-enhanced polymer (iAEP) technique has recently been developed that enables reliable immunohistochemistry-based detection of *ALK* fusion products (4). However, this technique has only been performed in cell lines and in large, surgically resected specimens; thus, it remains unclear whether such methodology can be applied to small biopsy samples obtained from patients with advanced NSCLC.

Endobronchial ultrasound-guided transbronchial needle aspiration (EBUS-TBNA) is an established modality for the definitive diagnosis of mediastinal and hilar adenopathy in

Authors' Affiliations: [1]Division of Thoracic Diseases, Chiba Cancer Center, Chiba, Japan; [2]Division of Thoracic Surgery, Toronto General Hospital, University Health Network, University of Toronto, Canada; [3]Division of Surgical Pathology, Chiba Cancer Center, Chiba, Japan; [4] Division of Genetic Diagnosis, Chiba Cancer Center, Chiba, Japan; [5]Division of Functional Genomics, Jichi Medical University, Tochigi, Japan; [6]Division of Pathology, The Cancer Institute, Japanese Foundation for Cancer Research, Tokyo, Japan; and [7]Department of General Thoracic Surgery, Graduate School of Medicine, Chiba University, Chiba, Japan

Corresponding Author: Takahiro Nakajima, Division of Thoracic Diseases, Chiba Cancer Center, 666-2 Nitona-cho, Chuo-ku 260-8717, Chiba, Japan. Phone: 81-43-264-5431; Fax: 81-43-262-8680; E-mail: nakajii@fc.med.miyazaki-u.ac.jp.

doi: 10.1158/1078-0432.CCR-10-0099

Translational Relevance

Acquisition of proper tissue samples for molecular analysis is not always an easy task; however, information obtained from such specimens is essential for the selection of appropriately targeted cancer therapies. This study shows that endobronchial ultrasound-guided transbronchial needle aspiration (EBUS-TBNA) contributes to the resolution of this issue in lung cancer because tissue samples obtained by EBUS-TBNA can be successfully used to assess the presence of echinoderm microtubule–associated protein-like 4–anaplastic lymphoma kinase fusion genes. We have shown that EBUS-TBNA samples could be subjected to immunohistochemistry, fluorescent *in situ* hybridization, and reverse transcription-PCR analysis. EBUS-TBNA for the assessment of mediastinal and hilar adenopathy is a practical tool that can be used in the molecularly targeted treatment era for lung cancer.

patients with lung cancer (5, 6). EBUS-TBNA is generally accepted to be as safe as standard bronchoscopy, less invasive than mediastinoscopy, and of high diagnostic quality. Compared with conventional fine-needle aspiration, EBUS-TBNA is an outstanding procedure with respect to its extremely low morbidity and its repeatability; fine-needle aspiration could cause pneumothorax, and repeated sampling might be difficult to perform.

In this study, we analyzed the feasibility of EBUS-TBNA for the detection of *EML4-ALK* fusion genes. We also retrospectively analyzed the clinicopathologic characteristics of *ALK*-positive lung cancer cases with mediastinal and/or hilar lymph node metastasis.

Materials and Methods

Patients

From April 2008 to July 2009, 112 cases with proven hilar and/or mediastinal lymph node metastasis of NSCLC were enrolled; re-sliced specimens for histologic examination were available for 109 of these cases. Independent pathologists (D. Ikebe and M. Itami) reviewed all cases and histologically confirmed the presence of cancer cells in each specimen. Morphologic features detected with H&E staining were also recorded, and mucin production was evaluated by Alcian blue staining. First, samples were screened for *ALK* abnormalities using immunohistochemistry. Cases that were determined to be *ALK*-positive or suspicious by immunohistochemistry in our laboratory were subjected to additional evaluation by FISH and immunohistochemistry restaining by an independent pathologist (K. Takeuchi) at the Division of Pathology, The Cancer Institute, Japanese Foundation for Cancer Research. Final confirmation was performed by direct sequencing of *EML4-ALK* fusion cDNAs using EBUS-TBNA histologic cores that had been preserved at −80°C. *EGFR* gene mutation status was also evaluated in all EBUS-TBNA samples. Associations between the presence of *ALK* fusion genes and clinicopathologic characteristics were retrospectively analyzed from medical records.

EBUS-TBNA

In all cases, chest computed tomography was performed prior to EBUS-TBNA. Brain magnetic resonance imaging, enhanced computed tomography, and bone scintigraphy were also performed for clinical staging of each case. EBUS-TBNA was performed for lymph nodes >5 mm in short axis on chest computed tomography. To obtain a histologic core, a dedicated 22-gauge needle equipped with an internal stylet was used. After the initial puncture, the internal stylet was used to clean out the internal lumen that was clogged with bronchial tissue (Fig. 1A). The internal stylet was removed, and negative pressure was applied using a syringe. The needle was then moved back and forth inside the lymph node. Finally, the needle was retrieved, and the internal stylet was used to push out the histologic core (6). Each histologic core was divided into two samples: one was fixed with formalin and used for histologic diagnosis, and the other was mixed with Allprotect Tissue Reagent (Qiagen) following the instructions of the manufacturer, and stored at −80°C.

ALK detection with immunohistochemistry

For detection of the *ALK* fusion gene, we applied the iAEP method, which incorporates an intercalating antibody between the primary antibody to *ALK* and dextran polymer–based detection reagents (4).

Histologic cores obtained by EBUS-TBNA were routinely fixed in 20% neutralized formalin and embedded in paraffin. Blocks were sliced at a thickness of 4 μm, and sections were placed on silane-coated slides. Antibody preparations specific for the intracellular region of *ALK* (5A4, Abcam) were subjected to immunohistochemical staining according to standard protocols using dextran polymer reagents (anti-mouse immunoglobulin, EnVision+DAB System; Dako). The *ALK* antibody (5A4) was used at a dilution of 1:50. For antigen retrieval and deparaffinization, slides were heated for 20 minutes at 98°C in Target Retrieval Solution (low pH; Dako) with PT-link (Dako). Pretreated slides were positioned in a programmable AutoStainer instrument (EnVision System; Dako). Following the immunohistochemical program, slides were incubated at room temperature first with Peroxidase Blocking Solution (Dako) for 5 minutes and then with *ALK* antibody (5A4, 1:50; Abcam) for 30 minutes. Following application of the iAEP method, which has been described in detail elsewhere (4), we included an incubation step of 15 minutes at room temperature with intercalated immunoglobulin (Mouse-LINKER; Dako) to increase the detection sensitivity. Immune complexes were then detected using the dextran polymer reagent for 30 minutes. 5A4-positive cells were stained with 3,3′-diaminobenzidine for 5 minutes, and nuclei were then stained with hematoxylin for 2 minutes.

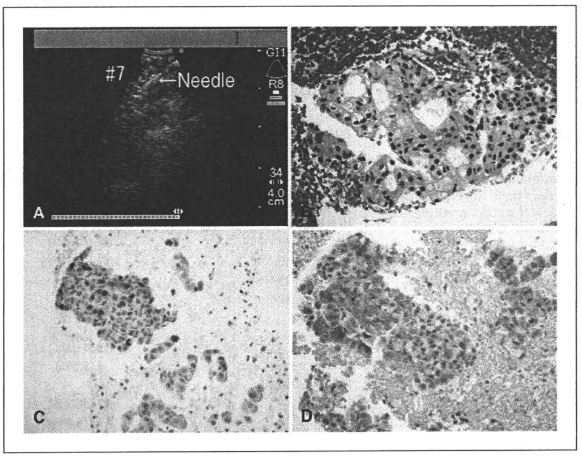

Fig. 1. Diagnosis of metastatic nodes by EBUS-TBNA. A, lymph node sampling by EBUS-TBNA. B, adenocarcinoma was revealed in the EBUS-TBNA sample. C, mucin production was observed by Alcian blue staining. D, immunohistochemistry with an anti-*ALK* antibody showed *ALK* fusion protein positivity in lung adenocarcinoma cells.

The samples obtained with EBUS-TBNA were small, paraffin-embedded biopsy specimens, which might limit the utility of immunohistochemistry. To avoid false-negative diagnosis, the first immunohistochemical procedure was used as a screening test to define three categories with which to judge the first run. Cancer cells were defined as "positive" if staining was as strongly positive as a positive control (clinical lung cancer tissues previously defined as positive by both molecular and immunohistochemistry analyses) and a fine, granular cytoplasmic staining pattern was observed. Cancer cells that showed no staining were classified as "negative." The "suspicious" classification was defined as the presence of weakly stained cells that were considered difficult to differentiate from background staining. While using these categories, we further subdivided the suspicious category into "probably positive" and "probably negative" categories. Probably positive meant that the tumor cells stained, but not strongly, whereas probably negative indicated very weak staining that was difficult to differentiate from background staining. After the screening immunohistochemistry, suspicious cases were re-tested by immunohistochemistry in addition to FISH by a second independent pathologist (K. Takeuchi).

Fluorescence *in situ* hybridization

To further confirm the *ALK* genomic rearrangement, two FISH assays were performed: an *ALK* split assay and an *EML4-ALK* fusion assay. Unstained sections were processed with a Histology FISH Accessory Kit (Dako), subjected to hybridization with fluorescently-labeled bacterial artificial chromosome clone probes for *EML4* and *ALK* (self-produced probes; *EML4* RP11-996L7, *ALK* RP11-984I21, and RP11-62B19) or for genomic regions upstream and downstream of the *ALK* breakpoint (Dako), stained with 4,6-diamidino-2-phenylindole, and examined with a fluorescence microscope (BX51; Olympus; ref. 7). FISH analysis was performed at the Division of Pathology, The Cancer Institute, Japanese Foundation for Cancer Research (K. Takeuchi). The FISH positivity criteria for EBUS-TBNA samples were defined as "over 50% cancer cells." As EBUS-TBNA samples are small biopsy samples, entire tumor cells in the paraffin-embedded section were evaluated.

RT-PCR and direct sequencing

Frozen histologic cores obtained by EBUS-TBNA were used to extract RNA. All immunohistochemistry-positive or suspicious cases were subjected to direct sequencing of the fusion cDNAs. RNA was extracted from frozen samples using the AllPrep DNA/RNA mini kit (Qiagen), and cDNA cloning was performed with the High Capacity RNA-to-cDNA Kit (Applied Biosystems). For RT-PCR analysis of *EML4-ALK*, we used primer sequences that have been described previously (2). After PCR amplification, PCR products were analyzed using agarose gel electrophoresis. RT-PCR products were extracted from gel slices using the QIAquick Gel Extraction Kit (Qiagen). Purified products were then sequenced with a capillary sequencer. Resultant nucleotide sequences were compared with previously reported sequences for determination of the *EML4-ALK* variant. *EGFR* mutation status was also examined using the peptide nucleic acid/locked nucleic acid PCR clamp method for samples obtained with EBUS-TBNA (8).

Ethics committee approval

This research was approved by the Ethics Committee of Chiba Cancer Center (nos. 20-21 and 21-10). Written consent was obtained from all patients. All samples were coded and managed independently.

Statistical analysis

For clinical characteristics and genetic factors, frequency analysis was performed with Fisher's exact test (dichotomous factors) and χ^2 test (multinomial factors). Mann-Whitney *U* test was applied to continuous data. General data analysis was conducted with StatView 5.0 (SAS Institute, Inc.). All *P* values were based on a two-sided hypothesis, $P < 0.05$ was considered to have statistical significance.

Results

Patient characteristics

The clinical characteristics of all 109 patients are listed in Table 1; 82 patients (75.2%) were male. The median age was 64.4 years (range, 38–90 y). Histologic examination was performed in all cases, leading to a diagnosis of adenocarcinoma (Fig. 1B) in 82 cases (75.2%), squamous cell carcinoma in 18 cases, and "other" in 9 cases. With respect to smoking status, 22 cases (20.4%) were never-smokers, 15 (13.9%) were light smokers (defined as a smoking index score <400), and 72 were heavy smokers (smoking index score ≥400). A total of 191 mediastinal lymph nodes and 84 hilar lymph nodes (2.52 lymph nodes/patient) were detected with EBUS, and 158 mediastinal lymph nodes and 71 hilar lymph nodes (2.10 lymph nodes/patient) were sampled. The median size of the sampled lymph nodes was 12.1 mm (range, 3.0–33.4 mm) in the short axis on ultrasound. According to criteria from the International Union Against Cancer, there were 9 stage II cases, 49 stage III cases, and 45 stage IV cases; the remaining 6 cases were defined as having recurrent lung cancer. *EGFR* gene mutations were detected in 25 cases (22.9%), which included 9 cases with in-frame deletions at exon 19, 9 cases with a point mutation at exon 21, 3 cases with a point mutation at exon 18, 2 cases with point mutations at exons 18 and 21, 1 case with a point mutation at exon 20, and 1 case with point mutations in exons 20 and 21.

Table 1. Clinical characteristics of patients with NSCLC

Parameter	Number of cases (%)
	109
Age	
Mean (y)	64.4 (range, 38–90)
Gender	
Male	82 (75.2%)
Female	27 (24.8%)
Pathology	
Adenocarcinoma	82 (75.2%)
Squamous cell	18 (16.5%)
Other histology	9 (8.3%)
Clinical stage	
II	9 (8.3%)
III	49 (45.0%)
IV	45 (41.3%)
Recurrence	6 (5.5%)
Bone metastasis	
Yes	22 (20.2%)
No	87 (79.8%)
Brain metastasis	
Yes	16 (14.7%)
No	93 (85.3%)
Smoking	
Never (SI = 0)	22 (20.4%)
Light (SI < 400)	15 (13.9%)
Heavy (SI ≥ 400)	70 (64.8%)
EGFR mutation status	25 (22.9%)
Exon 18	3
Exon 19	9
Exon 20	1
Exon 21	9
Exons 18 + 21	2
Exons 20 + 21	1

Abbreviation: SI, smoking index.

ALK fusion gene assessment

Out of 109 cases examined by immunohistochemistry using the iAEP method, 6 *ALK*-positive cases and 17 suspicious cases (1 probably positive and 16 probably negative) cases were detected. The staining of the small histologic core did not show any heterogeneity.

FISH confirmed the existence of an *ALK* fusion gene in all six *ALK*-positive cases (Figs. 1D, 2A and B), and there were no false-positive cases for immunohistochemistry. Sixteen probably negative cases were determined to be negative for the *ALK* fusion gene by re-testing with immunohistochemistry and FISH. One probably positive case had too few tumor cells to be used for FISH analysis; however, RT-PCR assessment confirmed the presence of *EML4-ALK* fusion cDNA. *EML4*, *ALK*, and fusion signals (arrows in Fig. 2A) are presented in the green, red, and merged image and a pair of split signals (arrow in Fig. 2B, downstream) shows rearrangement of *ALK*. In Fig. 2C, unique bands in each *ALK*-positive case reveal variant 1 and variant 3 *EML4-ALK* fusion genes. Thus, the *ALK* fusion gene was detected in a total of seven cases (6.4%). Direct sequencing of the PCR products revealed that four cases carried *EML4-ALK* variant 1, whereas three cases had variant 3. The fusion point of *ALK* and *EML4* is observed in the cDNA sequence (arrow in Fig. 2D).

Clinicopathologic characteristics of lung cancers possessing *ALK* fusion genes

Clinicopathologic characteristics were compared between the 7 *ALK*-positive cases and the 102 *ALK*-negative

cases (Table 2). All *ALK*-positive cases had an adenocarcinoma histology and lacked *EGFR* gene mutations. With respect to smoking habits, six out of the seven *ALK*-positive cases were either never-smokers or light smokers (smoking index score <400). No significant difference in gender was observed between *ALK*-positive and *ALK*-negative patients; however, *ALK*-positive patients were significantly younger than *ALK*-negative patients (55.4 versus 65.0 years; $P = 0.0408$). No significant differences in the incidence of bone metastasis (9.1% versus 5.7%; $P = 0.64$) or brain metastasis (12.5% versus 5.4%; $P = 0.30$) were observed. Overall, the mean primary tumor diameter was 40.4 mm; interestingly, the mean primary tumor diameter of *ALK*-positive cases was 28.6 mm, which was significantly smaller than that of *ALK*-negative cases (41.9 mm; $P < 0.05$). Mucin production was significantly more frequently observed in *ALK*-positive cases as shown by Alcian blue staining (Fig. 1C; $P < 0.01$). Finally, among the 84 cases expressing wild-type *EGFR*, 8.3% (7 of 84) were *ALK*-positive.

Discussion

This is the first attempt and report about using EBUS-TBNA samples in the detection of *ALK* fusion genes, and is expected to have a major effect on the management of patients with lung cancer. EBUS-TBNA is an established procedure for the evaluation of mediastinal and hilar adenopathy in patients with lung cancer. It is as safe, as highly diagnostic, and less invasive than other diagnostic modalities (9–11). Biopsy samples obtained with EBUS-TBNA can be subjected to histologic as well as cytologic evaluation. Nonsurgical modalities for obtaining tumor specimens are particularly critical in lung cancer because many patients have advanced disease at the time of first presentation, and are therefore not eligible for radical surgery. In addition to histologic diagnosis and stage definition, EBUS-TBNA enables molecular analysis of biopsy samples, the clinical significance of which is growing as molecularly targeted strategies for NSCLC are becoming increasingly important. We have previously reported that metastatic lymph node samples obtained by EBUS-TBNA can be applied to multidisciplinary analyses (5), and the present study is the first report of successful analysis of *ALK* fusion genes, a newly identified genetic abnormality in NSCLC, with such specimens (2). However, the small size of the paraffin-embedded biopsy samples obtained from EBUS-TBNA might limit the utility of this methodology; thus, multidirectional analysis will be critical for microsampling methods such as EBUS-TBNA.

The reliability of the newly developed immunohistochemistry (iAEP) method for the detection of *ALK* fusion

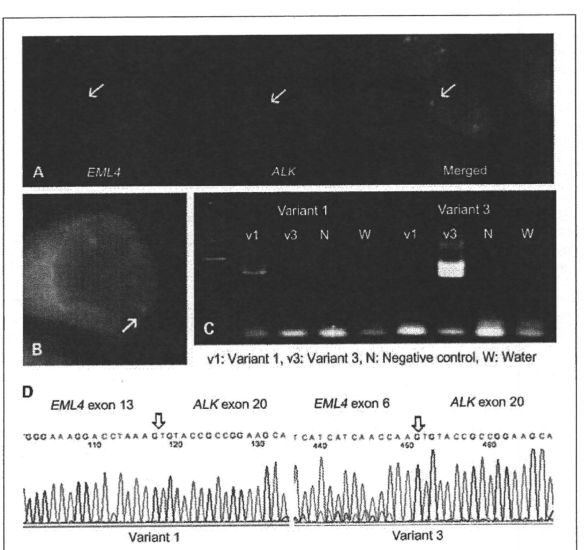

Fig. 2. Molecular analysis of *ALK* fusion genes. A, FISH *EML4-ALK* fusion assay with labeled probes for *EML4* (green, arrow) or *ALK* (red, arrow). The *EML4-ALK* fusion gene is observed (yellow, arrow). B, *EML4-ALK* split assay with labeled probes for the upstream (red) or downstream (green, arrow) region of the *ALK* locus. C, RT-PCR detection of the *EML4-ALK* fusion gene. D, direct cDNA sequence of *EML4-ALK* variants 1 and 3.

Table 2. Clinical, pathologic, and genetic analysis of *ALK*-positive NSCLC

Characteristic	*EML4-ALK* fusion			*P*
	NSCLC	+	−	
Female gender	27	4	23	0.062
Mean age (y)	64.4	55.4	65.0	0.0408
<60	29	5	24	0.0139
Bone metastasis	22	2	20	0.6396
Brain metastasis	16	2	14	0.2973
Mean tumor diameter (mm)	40.4	28.6	41.9	0.0478
Smoking index (n = 107)	784	161	827	0.0071
Never/light smoker	37	6	31	0.0056
Adenocarcinoma	82	7	75	0.1896
Mucin production	17	5	12	0.0009
EGFR wild-type	84	7	77	0.3317
ALK variant 1		4		
ALK variant 3		3		

NOTE: Two cases without primary tumors and six cases of recurrence were excluded from the tumor diameter analysis. Smoking history was recorded in 107 patients.

genes is very precise (4). This method is expected to be more practical for the detection of *ALK* fusion genes compared with FISH because FISH can sometimes be very difficult to perform for *ALK* fusion genes due to the close proximity of the two fusion gene components. We performed both fusion and split assays for FISH, and FISH was performed to confirm the immunohistochemical results. In addition, the *ALK* fusion genes are novel oncogenes in lung cancer. There is a possibility of existing unknown fusion pattern which cannot be detected by FISH or RT-PCR. Immunohistochemistry has an advantage of detecting novel unknown fusion patterns (4). In this study, we performed immunohistochemistry using the iAEP methodology and an Autostainer instrument. This technique is convenient, highly reproducible, and enables accurate diagnosis even if only a small amount of specimen is available. These features are well-suited for the screening of *ALK*-positive lung cancers using small biopsy samples. The Autostainer instrument also allows uniform immunohistochemical analysis, which may lead to consistent results among different institutions/hospitals; such uniformity is essential for the standardization of diagnostic procedures that assess the presence of *ALK* fusion genes. Recently, a highly sensitive antibody directed against *ALK* fusion products that can possibly be used for immunohistochemistry has been reported, therefore representing a novel candidate for *ALK* fusion detection (12).

The median age of *ALK*-positive cases in the present study was 55.4 years. Patients <60 years represent approximately 10% of all lung cancer deaths (6,655 of 63,255 deaths) according to the Japanese National Cancer Center Cancer Information Service Statistics published in 2008 (13). In the present study, a significant number of *ALK*-positive cases were <60 years of age (17.2%, 5 of 29; $P < 0.05$). *ALK*-positive cancer may therefore be more common in patients with early-onset NSCLC. However, it should be noted that two *ALK*-positive cases were >70 years of age (71 and 73 years); therefore, although patient age may become a predictor of *ALK* fusion gene positivity, *ALK* screening must also be performed in elderly individuals. The median diameter of primary lung tumors was significantly smaller in *ALK*-positive cases (28.6 versus 41.9 mm; $P < 0.05$), further emphasizing the importance of EBUS-TBNA because this technique does not require a large primary lesion. An additional advantage of EBUS-TBNA is that it can be used for lymph node sampling, which is relevant to the majority of advanced lung cancer cases. Although lung cancer is generally more common in smokers, most of the *ALK*-positive cases in this study (37 cases; 34.3%) were never-smokers or light smokers. The smoking index scores in the *ALK*-positive cohort were significantly lower than that of *ALK*-negative patients (161 versus 827; $P < 0.01$). Hence, being a never-smoker or light smoker seems to be a strong predictor of *ALK* positivity ($P < 0.01$).

Evaluation of the clinicopathologic characteristics of patients in our cohort indicated that *ALK*-positive lung cancer tends to have an adenocarcinoma histology, expresses wild-type *EGFR*, has an early age of onset (<60 y), manifests as a relatively small primary lesion, more frequently occurs in never-smokers or light smokers (smoking index score <400), and has a mucin-producing histology. However, as EBUS-TBNA samples are obtained from metastatic lymph nodes rather than the primary tumor, these clinical features are nearly compatible with previously reported features (14). Patients harboring one or more of these predictive factors may therefore derive the most benefit from *ALK* fusion gene screening.

Recently, *ALK*-positive NSCLC was reported to be a signet ring cell type adenocarcinoma (15, 16). We assume that this description also includes mucin production, i.e., mucin-producing tumors or tumors with >10% Alcian blue staining in the cytoplasm. Herein, we performed Alcian blue staining on suspected mucin-producing tumors as part of the histologic diagnosis. By this classification, 17 (15.6%) NSCLC cases were determined to be mucin-producing cancers. These cases were all adenocarcinomas and included five *ALK*-positive cases; thus, approximately 30% of the mucin-producing adenocarcinomas showed *ALK* positivity. This is a significantly high frequency compared with that of other NSCLCs ($P < 0.01$). This histologic feature, which can be assessed in cytologic samples, therefore seems to be useful for the prediction of *ALK* positivity.

The standard therapy for patients with advanced lung cancer at the time of presentation is chemotherapy and/or radiotherapy. However, standard platinum-based combined chemotherapy is not sufficient for disease eradication (17). Recently, lung cancer treatment strategies have become refined through the development of molecular markers and molecularly targeted agents. *ALK* inhibitors

have a high potential to become a definitive treatment for *ALK*-positive lung cancer, in a manner parallel to the exceptional therapeutic response of *EGFR*-positive lung cancers to *EGFR* tyrosine kinase inhibitors (18, 19). The efficacy of *ALK* inhibitors has been confirmed in cell lines (20, 21), and phase I clinical development of an oral *ALK* inhibitor for patients with lung cancer is currently under way (PF-02341066); two of the seven *ALK*-positive NSCLC cases from the present series have been enrolled in this trial (22, 23). As the background of *ALK*-positive lung cancer is similar to that of *EGFR*-positive lung cancer, and *ALK* tyrosine kinase inhibition is fundamentally similar to *EGFR* tyrosine kinase inhibition, *ALK* inhibitors might experience a similar progression of drug development and clinical and pathologic prediction of *ALK* positivity in lung cancer patients as *EGFR* tyrosine kinase inhibitors have for patients with *EGFR*-positive lung cancer. In this study, all *ALK*-positive lung cancers possessed wild-type *EGFR* and were therefore ineligible for *EGFR* tyrosine kinase inhibitor therapy (24). Therefore, *ALK* fusion gene assessment and administration of *ALK* inhibitors may become important for patients with *EGFR*-negative lung cancers.

Although some *ALK* inhibitors have already been developed and are currently being evaluated in clinical trials, it is important to establish a method for determining the existence of *ALK* fusion genes prior to the administration of *ALK* inhibitors. Both the presence of *ALK* fusion genes as well as *EGFR* gene mutations were successfully evaluated using histologic samples obtained by EBUS-TBNA of lung cancer regional lymph nodes. This diagnostic strategy allowed both pretreatment staging and evaluation of critical molecular markers to be definitively determined in a less invasive manner. There are some publications related with the genomic difference between primary tumor and metastatic site (25–29). EBUS-TBNA is a minimally invasive modality that allows the sampling of tumor cells from metastatic lymph node with a very low morbidity. The possibility of genetic differences should be considered whenever the biomarker information is used for the selection of patients for molecular target therapies. EBUS-TBNA is an ideal approach in this aspect.

In conclusion, EBUS-TBNA sampling is feasible for *ALK* fusion gene assessment by immunohistochemistry, FISH, and RT-PCR, as well as for pathologic diagnosis. The development of a safe and highly precise modality that enables the acquisition of a sufficient amount of high-quality tissue without surgery will become increasingly important in the molecularly targeted therapy era. EBUS-TBNA is one of the best candidates for such a methodology.

Disclosure of Potential Conflicts of Interest

K. Yasufuku, recipent of an unrestricted grant from Olympus Medical Corporation for Continuing Medical Education; H. Mano, member of the scientific advisory board, Pfizer Inc.

Acknowledgments

We thank Yuko Noguchi and Tetsushi Hirata for technical assistance with immunohistochemistry. We thank Drs. Yukiko Matsui, Masato Shingyoji, and Meiji Itakura for clinical analysis support. All authors have read and approved the final version of this manuscript.

Grant Support

This research was supported, in part, by the Ministry of Education, Culture, Sports, Science and Technology, Grant-in-Aid for Young Scientists (B) no. 21791340 in 2009 (T. Nakajima) and Grant-in-Aid for Cancer Research from Ministry of Health, Labor and Welfare in 2009 (T. Nakajima).

The costs of publication of this article were defrayed in part by the payment of page charges. This article must therefore be hereby marked *advertisement* in accordance with 18 U.S.C. Section 1734 solely to indicate this fact.

Received 01/14/2010; revised 06/14/2010; accepted 07/11/2010; published OnlineFirst 10/05/2010.

References

1. Mano H. Non-solid oncogenes in solid tumors: EML4-ALK fusion genes in lung cancer. Cancer Sci 2008;99:2349–55.
2. Soda M, Choi YL, Enomoto M, et al. Identification of the transforming EML4-ALK fusion gene in non-small-cell lung cancer. Nature 2007; 448:561–6.
3. Martelli MP, Sozzi G, Hernandez L, et al. EML4-ALK rearrangement in non-small cell lung cancer and non-tumor lung tissues. Am J Pathol 2009;174:661–70.
4. Takeuchi K, Choi YL, Togashi Y, et al. KIF5B-ALK, a novel fusion oncokinase identified by an immunohistochemistry-based diagnostic system for ALK-positive lung cancer. Clin Cancer Res 2009;15: 3143–9.
5. Nakajima T, Yasufuku K, Suzuki M, et al. Assessment of epidermal growth factor receptor mutation by endobronchial ultrasound-guided transbronchial needle aspiration. Chest 2007;132:597–602.
6. Yasufuku K, Chiyo M, Koh E, et al. Endobronchial ultrasound guided transbronchial needle aspiration for staging of lung cancer. Lung Cancer 2005;50:347–54.
7. Takeuchi K, Choi YL, Soda M, et al. Multiplex reverse transcription-PCR screening for EML4-ALK fusion transcripts. Clin Cancer Res 2008;14:6618–24.
8. Nagai Y, Miyazawa H, Huqun, et al. Genetic heterogeneity of the epidermal growth factor receptor in non-small cell lung cancer cell lines revealed by a rapid and sensitive detection system, the peptide nucleic acid-locked nucleic acid PCR clamp. Cancer Res 2005;65: 7276–82.
9. Yasufuku K, Chiyo M, Sekine Y, et al. Real-time endobronchial ultrasound-guided transbronchial needle aspiration of mediastinal and hilar lymph nodes. Chest 2004;126:122–8.
10. Herth FJ, Ernst A, Eberhardt R, Vilmann P, Dienemann H, Krasnik M. Endobronchial ultrasound-guided transbronchial needle aspiration of lymph nodes in the radiologically normal mediastinum. Eur Respir J 2006;28:910–4.
11. Herth FJ, Eberhardt R, Vilmann P, Krasnik M, Ernst A. Real-time endobronchial ultrasound guided transbronchial needle aspiration for sampling mediastinal lymph nodes. Thorax 2006;61:795–8.
12. Mino-Kenudson M, Chirieac LR, Law K, et al. A novel, highly sensitive antibody allows for the routine detection of ALK-rearranged lung adenocarcinomas by standard immunohistochemistry. Clin Cancer Res 2010;16:1561–71.
13. National Cancer Center Cancer Information Service. Available from: http://ganjoho.ncc.go.jp/public/statistics/backnumber/odjrh3000000vdf1-att/date02.pdf. Accessed on August 28, 2009.
14. Takahashi T, Sonobe M, Kobayashi M, et al. Clinicopathologic features of non-small-cell lung cancer with EML4-ALK fusion gene. Ann Surg Oncol 2010;17:889–97.

15. Inamura K, Takeuchi K, Togashi Y, et al. EML4-ALK fusion is linked to histological characteristics in a subset of lung cancers. J Thorac Oncol 2008;3:13–7.
16. Inamura K, Takeuchi K, Togashi Y, et al. EML4-ALK lung cancers are characterized by rare other mutations, a TTF-1 cell lineage, an acinar histology, and young onset. Mod Pathol 2009;22:508–15.
17. Wakelee H, Belani CP. Optimizing first-line treatment options for patients with advanced NSCLC. Oncologist 2005;10:1–10.
18. Lynch TJ, Bell DW, Sordella R, et al. Activating mutations in the epidermal growth factor receptor underlying responsiveness of non-small-cell lung cancer to gefitinib. N Engl J Med 2004;350: 2129–39.
19. Paez JG, Jänne PA, Lee JC, et al. EGFR mutations in lung cancer: correlation with clinical response to gefitinib therapy. Science 2004; 304:1497–500.
20. Koivunen JP, Mermel C, Zejnullahu K, et al. EML4-ALK fusion gene and efficacy of an ALK kinase inhibitor in lung cancer. Clin Cancer Res 2008;14:4275–83.
21. Piva R, Chiarle R, Manazza AD, et al. Ablation of oncogenic ALK is a viable therapeutic approach for anaplastic large-cell lymphomas. Blood 2006;107:689–97.
22. Kwak EL, Camidge DR, Clark J, et al. Clinical activity observed in a phase I dose escalation trial of an oral c-met and ALK inhibitor, PF-02341066. J Clin Oncol 2009;27:15s.
23. Christensen JG, Zou HY, Arango ME, et al. Cytoreductive antitumor activity of PF-2341066, a novel inhibitor of anaplastic lymphoma kinase and c-Met, in experimental models of anaplastic large-cell lymphoma. Mol Cancer Ther 2007;6:3314–22.
24. Shaw AT, Yeap BY, Mino-Kenudson M, et al. Clinical features and outcome of patients with non-small-cell lung cancer who harbor EML4-ALK. J Clin Oncol 2009;27:4247–53.
25. Kalikaki A, Koutsopoulos A, Trypaki M, et al. Comparison of EGFR and K-RAS gene status between primary tumours and corresponding metastases in NSCLC. Br J Cancer 2008;99:923–9.
26. Gow CH, Chang YL, Hsu YC, et al. Comparison of epidermal growth factor receptor mutations between primary and corresponding metastatic tumors in tyrosine kinase inhibitor-naive non-small-cell lung cancer. Ann Oncol 2009;20:696–702.
27. Daniele L, Cassoni P, Bacillo E, et al. Epidermal growth factor receptor gene in primary tumor and metastatic sites from non-small cell lung cancer. J Thorac Oncol 2009;4:684–8.
28. Park S, Holmes-Tisch AJ, Cho EY, et al. Discordance of molecular biomarkers associated with epidermal growth factor receptor pathway between primary tumors and lymph node metastasis in non-small cell lung cancer. J Thorac Oncol 2009;4:809–15.
29. Schmid K, Oehl N, Wrba F, et al. EGFR/KRAS/BRAF mutations in primary lung adenocarcinomas and corresponding locoregional lymph node metastases. Clin Cancer Res 2009;15:4554–60.

INTERNAL MEDICINE

□ CASE REPORT □

Incidentally Proven Pulmonary "ALKoma"

Atsushi Osoegawa[1], Kaname Nosaki[1], Hitoshi Miyamoto[1], Takuro Kometani[1], Fumihiko Hirai[1], Kaoru Ondo[1], Takashi Seto[1], Kenji Sugio[1], Young Lim Choi[2], Manabu Soda[2], Hiroyuki Mano[2] and Yukito Ichinose[1]

Abstract

Genetic alterations of echinoderm microtubule-associated protein-like 4 (*EML4*)-anaplastic lymphoma kinase (*ALK*) inversion were recently found in lung cancer. A 39-year-old woman with multiple brain metastases and bulky mediastinal lymph node metastases was admitted. Biopsy from her supraclavicular lymph nodes was performed to differentiate the diagnosis between lymphoma and lung cancer. Pathologically, the lymph nodes had a feature of adenocarcinoma. On the other hand, the commercially available chromosomal fluorescent in situ hybridization (FISH) analysis showed split signals of *ALK*, which was confirmed to be the *EML4-ALK* inversion. The commercial-based ALK FISH is useful for screening pulmonary ALKoma.

Key words: EML4-ALK, lung cancer, oncogene addiction

(Inter Med 49: 603-606, 2010)
(DOI: 10.2169/internalmedicine.49.3126)

Introduction

The echinoderm microtubule-associated protein-like 4 (*EML4*)-anaplastic lymphoma kinase (*ALK*) inversion was recently detected in 6.7% of Japanese non-small cell lung cancer (NSCLC) patients (1). The fusion gene encodes a constitutive active oncoprotein with activated ALK kinase, resulting in the aberrant activation of the downstream signaling targets including Akt, signal transducer and activator of transcription (STAT) 3, and Ras-extracellular signal-regulated kinase (ERK) 1/2 (2).

The term ALKoma, coined by Benharroch et al, originally was used to represent anaplastic large cell lymphoma (ALCL) carrying the t(2 ; 5)(p23 ; q35) chromosome translocation (3). In 1994, Morris et al found that the t(2 ; 5) translocation fuses part of the nucleophosmin (*NPM*) gene on chromosome 5q35 to a portion of the ALK receptor tyrosine kinase gene on chromosome 2p23 (4). As with other fusion proteins found in hematological malignancies, ALKoma is also thought to become addicted to the ALK signaling pathway (3). Recently oncogene addiction has mainly been recognized among non-smoking NSCLC patients (5, 6). Just as epidermal growth factor receptor (*EGFR*) tyrosine kinase inhibitors (TKIs) have become a mainstay of therapy for patients harboring *EGFR* mutation, patients with *EML4-ALK* inversion may benefit from therapy with ALK inhibitors. We herein report an incidentally proven *EML4-ALK* inversion in primary pulmonary adenocarcinoma.

Abbreviations: EML4: echinoderm microtubule-associated protein-like 4, ALK: anaplastic lymphoma kinase, NSCLC: non-small cell lung cancer, ALCL: anaplastic large cell lymphoma, NPM: nucleophosmin, EGFR: epidermal growth factor receptor

Case Report

A 39-year-old woman was admitted to hospital because of generalized seizures. An initial screening head and body CT showed multiple brain metastases and swelling lymph nodes throughout the thorax (Fig. 1A, B). Fiber optic bronchoscopy showed direct invasion of tumor to the carina (Fig. 1C). After a crisis of generalized seizures, neurological disorders were not obvious. The patient's performance status (PS) was graded as one, because of a dry cough, which had

[1]Department of Thoracic Oncology, National Kyushu Cancer Center, Fukuoka and [2]Division of Functional Genomics, Jichi Medical University, Tochigi
Received for publication November 9, 2009; Accepted for publication December 15, 2009
Correspondence to Dr. Atsushi Osoegawa, osoegawa-ths@umin.ac.jp

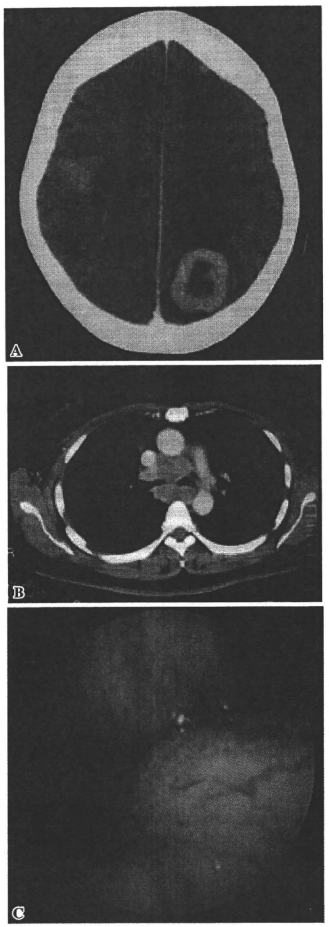

Figure 1. The imaging at presentation. Computed tomography presents multiple brain metastases (A) and mediastinal lymphadenopathy (B). Fiber optic bronchoscopy showed a direct invasion from metastatic lymph nodes to the carina (C). Both bronchi are too narrow to perform further examinations.

been apparent for the past 6 months before her admission to our hospital. Fine needle aspiration was performed from her right supraclaviclar lymph nodes, and malignancy at any origin was detected. As the patient was suspected to have malignant lymphoma or lung neoplasm, she was transferred to our institution for further examinations and therapies.

The laboratory data, including the tumor markers (carcinoembrionic antigen and soluble interleukin 2 receptor) were normal. The white blood cell count was 11,770/μL, probably due to the prophylactic use of corticosteroids against seizures. As the patient was thought to be in need of immediate therapy, an open biopsy from her right supraclavicular lymph nodes under local anesthesia was performed on the day of the transfer. The frozen samples were subjected to pathological examination, to *EGFR* mutation analysis (the peptide nucleic acid-locked nucleic acid polymerase chain reaction (PCR) clamp method (7), Mitsubishi Chemical Medience, Tokyo, Japan), and to a comprehensive analysis for malignant lymphoma. Pathologically, the lymph nodes had a feature of moderately to poorly differentiated adenocarcinoma (Fig. 2A), with positive immunohistochemical staining for thyroid transcription factor-1 and epithelial markers (CAM5.2 and AE1/AE3). Immunohistochemical staining for lymphocyte markers was negative (CD20, CD45 RO, and CD30). Finally, her clinical diagnosis was determined to be cTxN3M1(BRA), clinical stage IV, adenocarcinoma of the lung. Although she was a young, never-smoking Japanese woman (8), she was found to be negative for *EGFR* mutations.

Meanwhile, the results of a comprehensive analysis for malignant lymphoma were reported. These analyses consisted of flow cytometric analyses with CD45 gating and a chromosomal G-banding analysis. In addition, the chromosomal fluorescent in situ hybridization (FISH) analyses were performed to detect the transition of *ALK* (2p23), *BCL6* (3q27), *IGH/BCL1* t(11 ; 14)(q13 ; q32), *IGH/BCL2* t(14 ; 18)(q32 ; q21), and *IGH/CMYC* t(8 ; 14)(q24 ; q32), based on a pathologist's decision ("ML-NET", SRL, Tokyo). In this case, the FISH analyses were added because the sample was not adequate for G-banding. Surprisingly, the FISH analysis of *ALK*, using 5′-(green) and 3′-(red) sequences for hybridization probes, showed the split signals of *ALK*, in up to 96% of the cells counted (total 100 cells) (Fig. 2B). In order to analyze the counterpart of transition for *ALK*, multiplex reverse transcription PCR of the EML4-ALK fusion transcripts was performed by YLC, MS and HM, and the transition was found to be EML4-ALK inversion, variant 2 (Fig. 2C).

Abbreviations: PCR: polymerase chain reaction, FISH: fluorescent in situ hybridization

Discussion

EML4-ALK inversion was first identified by Soda et al, from a lung adenocarcinoma specimen that was surgically resected from a 62-year-old male with a history of smoking. They made a cDNA library from the specimen, inserted cDNAs into the plasmid clones, and then infected them into mouse 3T3 fibroblasts with recombinant retrovirus to assess its ability to transform the foci. *The EML4-ALK* inversion transcripts were found in one of the transformed foci (1).

ALK, as well as leukocyte tyrosine kinase (*LTK*), is a re-